이학박사 학위논문

KRAS 돌연변이 대장암세포주에서 분비된 MIF가 세툭시맙 내성에 미치는 기전 연구

Mutant KRAS-induced Macrophage Migration Inhibitory Factor (MIF) secretion promotes resistance to cetuximab in colorectal cancer

2018년 08월

서울대학교 대학원

협동과정 종양생물학 전공

장 지 은

KRAS 돌연변이 대장암세포주에서 분비된 MIF가 세툭시맙 내성에 미치는 기전 연구

지도교수 김 태 유

이 논문을 이학박사 학위논문으로 제출함

2018년 07월

서울대학교 대학원

협동과정 종양생물학 전공

장 지 은

장 지 은의 이학박사 학위논문을 인준함

2018년 08월

위 원 장 _____ (인)

부위원장 _____ (인)

위 원 _____ (인)

위 원 _____ (인)

위 원 _____ (인)

Mutant KRAS-induced Macrophage Migration Inhibitory Factor (MIF) secretion promotes resistance to cetuximab in colorectal cancer

By

Jee-Eun Jang

(Directed by Tae-You Kim, M.D., Ph.D.)

A Thesis Submitted in Partial Fulfillment of the Requirements for the Degree of Doctor of Science in Cancer Biology at the Seoul National University, Seoul, Korea

August 2018

Approved by thesis committee:

Professor _____ **Chairperson**

Professor _____ **Vice Chairperson**

Professor _____

Professor _____

Professor _____

ABSTRACT

Mutant KRAS-induced Macrophage Migration Inhibitory Factor (MIF) secretion promotes resistance to cetuximab in colorectal cancer

Jee-Eun Jang

Major in Cancer Biology

Department of cancer biology

The Graduate School

Seoul National University

The tumor microenvironment is recognized as a developing crosstalk between different cells by secretion of growth factors and cytokines thus providing oncogenic signals enhancing tumor progression and drug resistance. Here, I hypothesized that tumor cells carrying KRAS mutation-induced cytokines may

have critical roles in intercellular communication between microenvironment and tumor cells. I first investigated biological evidence of secreted cytokines in KRAS mutant-type ($KRAS^{MT}$) cell lines. I explored the roles of cytokine that cell morphology, proliferation, colony formation, wound healing, and invasion ability were enhanced when KRAS wild-type ($KRAS^{WT}$) cells were exposed to conditioned media (CM) from $KRAS^{MT}$ cells and I found macrophage migration inhibitory factor (MIF) was highly expressed in $KRAS^{MT}$ cells by analysis of proteomics. I also observed secreted MIF level between $KRAS^{WT}$ and $KRAS^{MT}$ cells, and it was highly secreted in $KRAS^{MT}$ cells. In addition, compared with colorectal cancer patients whose KRAS mutation was not harbored, MIF expression was higher in patients who have KRAS mutation. The predictive marker of KRAS mutation in colorectal cancer patients is associated with resistance to anti-epidermal growth factor receptor (EGFR) antibodies cetuximab (CTX). Following the hypothesis, I investigated that secreted cytokines from $KRAS^{MT}$ cells have an effect on the cetuximab resistance to the surrounding cells including $KRAS^{WT}$ cells. Treatment of CM led to cetuximab resistance in $KRAS^{WT}$ cells and MIF blockade prevented cetuximab resistance. Moreover, CM from MIF knocked out $KRAS^{MT}$ cells by using CRISPR/Cas9 system resulted in sensitizing to cetuximab resistance compared with treatment of CM from $KRAS^{MT}$ cells.

In conclusion, I demonstrated for the first time that MIF promoted the

cetuximab resistance of $KRAS^{WT}$ colorectal cancer cells, and this effect was mediated by paracrine and autocrine signaling-induced activation of the intracellular AKT signaling pathways and regulated by NF-kB transcription factor through oncogenic KRAS mutation. These findings suggest that MIF may be a promising predictive biomarker for the cetuximab resistance of KRAS wild-type colorectal cancer patients.

Keywords : Colorectal cancer, KRAS mutation, cytokine, cetuximab, MIF

Student Number : 2014-31287

TABLE OF CONTENTS

LIST OF FIGURES

INTRODUCTION

Colorectal cancer (CRC) is the third most common cancer and leading cause of cancer-related deaths in the world [1]. Diverse number of oncogenes and tumor suppressor genes which most prominently the APC, KRAS, and p53 genes are mutated in CRCs [2]. CRC also shows a very heterogeneous disease and that molecular and genetic features of the tumor determine the prognosis and response to targeted therapy [3]. KRAS alteration was found in non-hypermutated tumors with 55% rate in colorectal cancer [4]. KRAS gene mutations, in codons 12 and 13 of exon 2, lead to constitutive activation of the MAPK pathway, and are found in approximately 40% of patients with metastatic CRC [5, 6]. Oncogenic mutations in KRAS drive tumor growth by engaging multiple downstream mitogenic pathways, including RAF-MAPK and PI3K-AKT [7]. High concordance is also reported between KRAS mutations from primary tumors and metastases [8], suggesting to KRAS mutation early in the adenoma–carcinoma cascade. The ability to analyze the sequence of all protein-encoding genes in cancers has shown that the variety of mutations in cancers, showing the heterogeneity and complexity of human cancer [9]. Following reported data, they found that the probability and heterogeneity of populations with drug-resistant phenotypes increased drastically in tumor [10, 11].

Cetuximab (CTX), a monoclonal antibody that binds the extracellular domain

of EGFR, is effective in a subset of KRAS wild-type metastatic colorectal cancer [12]. It was reported that the presence of KRAS G12-, G13-, and Q61-mutations in tissue biopsies from patients with colorectal cancer who relapse after EGFR-targeted therapies [13]. Despite KRAS mutations were not detected in tumor tissues, tumor tissues contain variable cell population harboring mutations as showing tumor heterogeneity [14-16]. Cancer cells and their associated stroma coexist in a soluble factor including cytokine regulating their interaction in tumor microenvironments. Substantial evidence suggests that mechanisms that involve the tumor microenvironment also mediate resistance of tumors to chemotherapy. Cytokine-mediated signaling interactions between cells induce the protection from therapy and shows complex acquired drug resistance [17]. In tumor microenvironments, cytokines are strongly implicated in the development of cancer. Certain cytokines promote the development of a pro-tumorigenic microenvironment by recruitment of immune cells, as well as having direct effects on tumor, endothelial and stromal cells in order to promote cancer development and progression [18].

Macrophage migration inhibitory factor (MIF) is one of the first cytokines to be discovered. MIF gene promotes the inflammatory process through its activity as a chemokine and is also capable of promoting cell migration indirectly by stimulating other cells by paracrine signaling [19]. These secreted MIF gene is

potentially contribution of tumor development and progression, through the promotion of inflammation, direct effects on the tumor stroma [20]. In addition, the reported data showed that analysis of human colon cancer tissues demonstrated that MIF expression was upregulated in the colonic adenocarcinoma [21, 22]. It may indicate the MIF expression in serum or cancer tissue may have possibility for both the diagnosis and prognostication of colon cancer.

I hypothesized that the cytokine MIF, which KRAS mutant-induced, secreted from $KRAS^{MT}$ cells may have critical roles in intercellular communication between microenvironment and tumor cells as led to characteristics for tumorigenesis and cetuximab resistance to surrounding $KRAS^{WT}$ cells.

MATERIALS AND METHODS

Cell lines and reagents

Human CRC cell lines were obtained from the Korean Cell Line Bank (Seoul, Korea) or American Type Culture Collection (Manassas, VA, USA;) [23] . Cells were cultured at 37°C in a humidified atmosphere with 5% CO2 and grown in RPMI-1640 or Dulbecco's modified Eagle's medium containing 10% fetal bovine serum (Gibco, Carlsbad, CA, USA) and 50 μg/mL gentamicin. 4-IPP was purchased from Selleck Chemicals (Houston, TX, USA). Stock solutions were prepared in dimethyl sulfoxide (DMSO) and stored at -20°C. Human recombinant MIF was purchased from Peprotech

Conditioned medium preparation

To prepare conditioned medium (CM), HCT-116 cells were seeded in a 150-mm culture dish. The cells were incubated in serum-free RPMI for 48hrs to produce CM. The CM was collected, centrifuged at 500 g for 5 min, filtered through a 0.45-μm filter to remove cellular debris, and finally stored at -80°C until use.

Cell proliferation assays

The viability of cells was assessed by MTT assays (Sigma-Aldrich, St Louis, MO, USA). A total of 6×10^3 cells/well for DiFi to 1×10^4 cells/well for NCI-H508 were seeded in 96-well plates, incubated for 24hrs, and then treated for 72hrs with the indicated drugs at 37°C. After the treatments, MTT solution was added to each well, followed by incubation for 4hrs at 37°C. The medium was removed, and then DMSO was added, followed by thorough mixing for 10 min at room temperature. Cell viability was determined by measuring absorbance at 540nm using a VersaMax microplate reader (Molecular Devices, Sunnyvale, CA, USA). The concentrations of drugs required to inhibit cell growth by 50% (IC50) was determined using GraphPad Prism (La Jolla, CA, USA). Six replicate wells were used for each analysis, and at least three independent experiments were conducted. The data from replicate wells are presented as the mean number of the remaining cells with 95% confidence intervals.

Protein extraction and western blotting

Antibodies against p-EGFR (pY1068), p-AKT (pS473), pERK1/2, p-S6 (pS240, 244), and p4E-BP were purchased from Cell Signaling Technology (Beverley, MA, USA). An anti-KRAS and anti-B-actin antibody were purchased from Santa Cruz Biotechnology (Santa Cruz, CA, USA). The anti-MIF antibody was purchased from R&D Systems (Minneapolis, MN, USA). Subconfluent cells (70–80%) were

used for protein analyses. The cells were treated under various conditions as described. Cells were lysed in RIPA buffer on ice for 15 min (50 mmol/L Tris-HCl, pH 7.5, 1% NP-40, 0.1% Na deoxycholate, 150 mmol/L NaCl, 0.1 mmol/L aprotinin, 0.1 mmol/L leupeptin, 0.1 mmol/L pepstatin A 50 mmol/L NaF, 1 mmol/L sodium pyrophosphate, 1 mmol/L sodium vanadate, 1 mmol/L nitrophenolphosphate, 1 mmol/L benzamidine, and 0.1 mmol/L PMSF) and centrifuged at 12000g for 20 min. Samples containing equal amounts of total protein were resolved in SDS polyacrylamide denaturing gels, transferred to nitrocellulose membranes, and probed with antibodies. Detection was performed using an enhanced chemiluminescence system (Amersham Pharmacia Biotech, Buckinghamshire, UK).

RT-PCR and quantitative real-time RT-PCR

Total RNA was extracted from each cell line for transcriptome sequencing using an RNeasy mini kit (Qiagen, Valencia, CA, USA) according to the manufacturer's instructions. The cDNA was synthesized from total RNA (1 μg) using ImProm-II™ reverse transcriptase (Promega, Madison, WI, USA) and amplified by RT-PCR using AmpliTaq Gold® DNA polymerase (Applied Biosystems, Foster City, CA, USA) with buffer supplied by the manufacturer and gene/fusion junction-specific primers. For quantitative real-time RT-PCR (qRT-

PCR), cDNA was amplified using Premix Ex Taq (TaKaRa, Shiga, Japan) with SYBR® Green I (Molecular Probes, Eugene, OR, USA) using a StepOnePlus™ Real-Time PCR system (Applied Biosystems).

Invasion assay

5×10^4 cells were seeded on the Matrigel-coated membrane matrix (BD) insert well according to manufacturer's instructions after 24hrs. CM was added as a chemoattractant to the wells of the Matrigel invasion chamber for 48hrs. The following day, the cells were fixed for 10 min in 3.7% PFA and the insert was washed with phosphate-buffered saline (PBS). Crystal violet (0.1%) was added to the insert for 30 min and washed twice with PBS, and then with water. A cotton swab was used to remove any non-invading cells and the insert was washed again. The number of invading cells was imaged using a microscope equipped with a digital camera.

ELISA (Enzyme-linked immunosorbent assay)

An ELISA for MIF was used to measure the secreted cytokine by CRC cells. The cells were incubated in serum-free medium for 48hrs. Culture supernatants were collected at the indicated times, and the amounts of secreted MIF in the supernatants were quantified using a commercially available ELISA kit (R&D

Systems, Minneapolis, MN, USA).

Plasmid constructs and transfection

MIF cDNA was purchased from the Korea Human Gene Bank (Daejeon, Korea). The primers used for cloning were as follows: MIF, forward primer 5′-GGCGAATTCATGCCGATGTTCATCGTAAACA-3′ (including a 5′ EcoRI site) and reverse primer 5′- GCCCTCGAGTTAGGCGAAGGTGGAGTTGTTC-3′ (including a 5′ XhoI site). The amplified fragments were cloned into the pCMV-Tag2B simple vector (Addgene, Cambridge, MA, USA). All resulting plasmids were verified by Sanger sequencing. Transient transfection was conducted using Lipofectamine 2000 (Invitrogen, Carlsbad, CA, USA), according to the protocol suggested by the manufacturer.

RNA interference

sgRNAs targeting MIF were designed using the genscript online tool (http://www.genscript.com). The following sgRNA sequences were used: forward primer 5′-CACCGGAGGAACCCGTCCGGCACGG-3′ and reverse primer 5′-AAACCCGTGCCGGACGGGTTCCTCC-3′. Oligos were annealed and cloned into the lentiCRISPR2 vector (Addgene, Cambridge, MA, USA) using a standard BsmBI protocol. All resulting plasmids were verified by Sanger sequencing. The

LentiCRISPR2 MIF knock-out construct was transfected into the HCT-116 cell line using Lipofectamine 2000 to generate stable cell lines through selection with puromycin.

2D colony formation assay

For each cell line, 1×10^4 cells were seeded in 6-well plates in duplicate. After 48hrs, media containing 4-IPP (20, 50, and 100 uM) and cetuximab (0, 0.1, 1, 10, and 100 μg/mL) were added. Cells were grown for 14 days at 37°C with 5% CO2. The cells were washed with ice-cold PBS and stained with 0.5% crystal violet in 25% methanol.

3D colony formation assay

5×10^2 cells were mixed with Matrigel and seeded with NM and CM in 12-well plates in triple. Cetuximab (0, 0.1, 1, 10, and 100 μg/mL) were added to the NM and CM. Cells were grown for 14 days at 37°C with 5% CO2. Spheroid formed cells were observed by microscopy.

Wound healing assay

For the cell migration assay, cells were seeded into a 6-well culture plate until 90% confluent. The cells were then maintained in serum-free medium for 12hrs.

The monolayers were carefully scratched using a 10 μl pipette tip. The cellular debris was subsequently removed by washing with PBS, and the cells were incubated in NM and CM. The cultures were photographed at 0 and 30hrs to monitor the migration of cells into the wounded area.

BrdU assay

The BrdU assay was performed to determine the effects of cetuximab on cell proliferation. Briefly, cover glasses were coated with poly-L-lycine (Sigma-Aldrich) by following protocol, 5×10^5 NCI-H508 cells were seeded after 10 minute. Then, 5×10^6 HCT-116 cells and NCI-H508 cells were seeded in 150 pie dishes. Next day, cover glasses were located to each of 150 pie dish, and 100 μg/mL cetuximab was treated for 48hrs. Thereafter, BrdU was treated for over night at 4 ℃ and the cells were washed 3 times with phosphate-buffered saline (PBS) and fixed in 3.8% formaldehyde for 20 minutes. The cells were incubated with 2% BSA in PBS for 1hrs at room temperature. After washing 3 times with PBS, immunofluorescence was performed to visualize incorporated BrdU by using a mouse anti-BrdU antibody (Santa Cruz Biotechnology) according to the manufacture's protocol and mounted in VECTASHIELD mounting medium with DAPI (Vector Laboratories, Burlingame, CA). An automated microscope (DMI6000B) was used to automatically visualize images of the cells

Luciferase assay

I used a dual-luciferase reporter assay system (Promega, Madison, WI, USA) to determine promoter activity. Briefly, cells were transfected with MIF luciferase reporter plasmid (Stratagene, Grand Island, NY, USA) using lipofectamine 2000 reagent (Invitrogen, Carlsbad, CA, USA) Indianapolis, IN, USA) according to the manufacturer's instructions. KRAS G12V and MIF plasmid was co-transfected. 48hrs after transfection, luciferase activity was assayed using the dual-luciferase assay kit (Promega) according to the manufacturer's instructions. Luminescence was measured with a GloMax™ 96 microplate luminometer (Promega).

Statistical analysis

Statistical significance of the results was calculated using an unpaired Student's t-test, with a Graphpad program. $P < 0.05$ was considered significant.

RESULTS

Conditioned medium from $KRAS^{MT}$ cells promotes the tumor progression in $KRAS^{WT}$ cells

First, I investigated the effects of tumorigenicity by conditioned media from $KRAS^{MT}$ cells to $KRAS^{WT}$ cells under poor conditions. HCT-116^{MT} and NCI-$H508^{WT}$ cells were cultured for 48hrs under serum deprivation stress and conditioned media (CM) and normal media (NM) were harvested from HCT-116^{MT} and NCI-$H508^{WT}$ cells, respectively (Figure 1). NCI-$H508^{WT}$ cells were cultured with NM and CM for 24hrs and 48hrs than I observed that cell morphology and growth rate were increased when cultured with CM compared with NM (Figure 2A). Also, I have confirmed that NCI-$H508^{WT}$ cells obtained highly increased anchorage-independent ability showing increase of colony diameter under CM treated condition at three-dimensional culture by using matrigel (Figures 2B and C). And I conducted wound healing assay with $DiFi^{WT}$ cells in a time dependent manner, wound healing ability was increased when CM was treated (Figures 2D). In addition, treatment of CM significantly increased invasion ability in $NIH3T3^{WT}$ cells (Figure 2E) and CCD-841-CoN^{WT} cells (Figure 2F). I conducted invasion assay by using human colorectal tumor organoid samples (Figure 2G). OGB017N human normal organoids showed increased invasion ability when CM from

OGB014T (patient carrying KRAS G12S mutation) was treated, compared with CM from OG050T (KRAS wild-type patient). These results showed the same effects with CM expressing KRAS endogenously.

These results suggested that $KRAS^{WT}$ cells, which are located around $KRAS^{MT}$ cells, were promoted cell proliferation, growth, wound healing, and invasive ability, which are characteristics for tumorigenecity, by treatments of CM from $KRAS^{MT}$ cells through cell to cell interaction in tumor microenvironment.

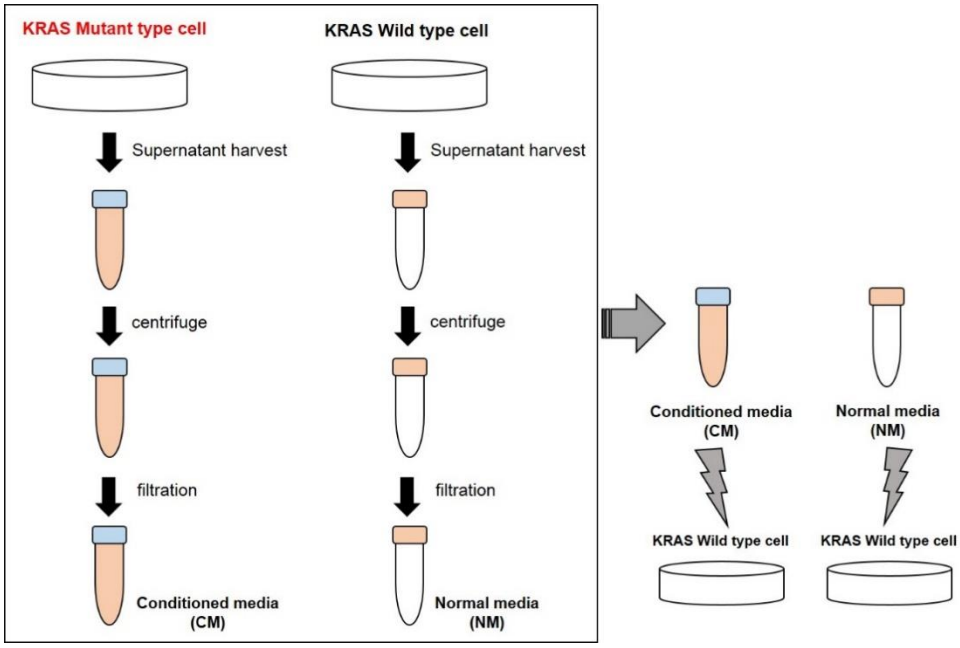

Figure 1. Schematic figure shows the production of conditioned media (CM) and normal media (NM) from $KRAS^{MT}$ cells and $KRAS^{WT}$ cells, respectively.

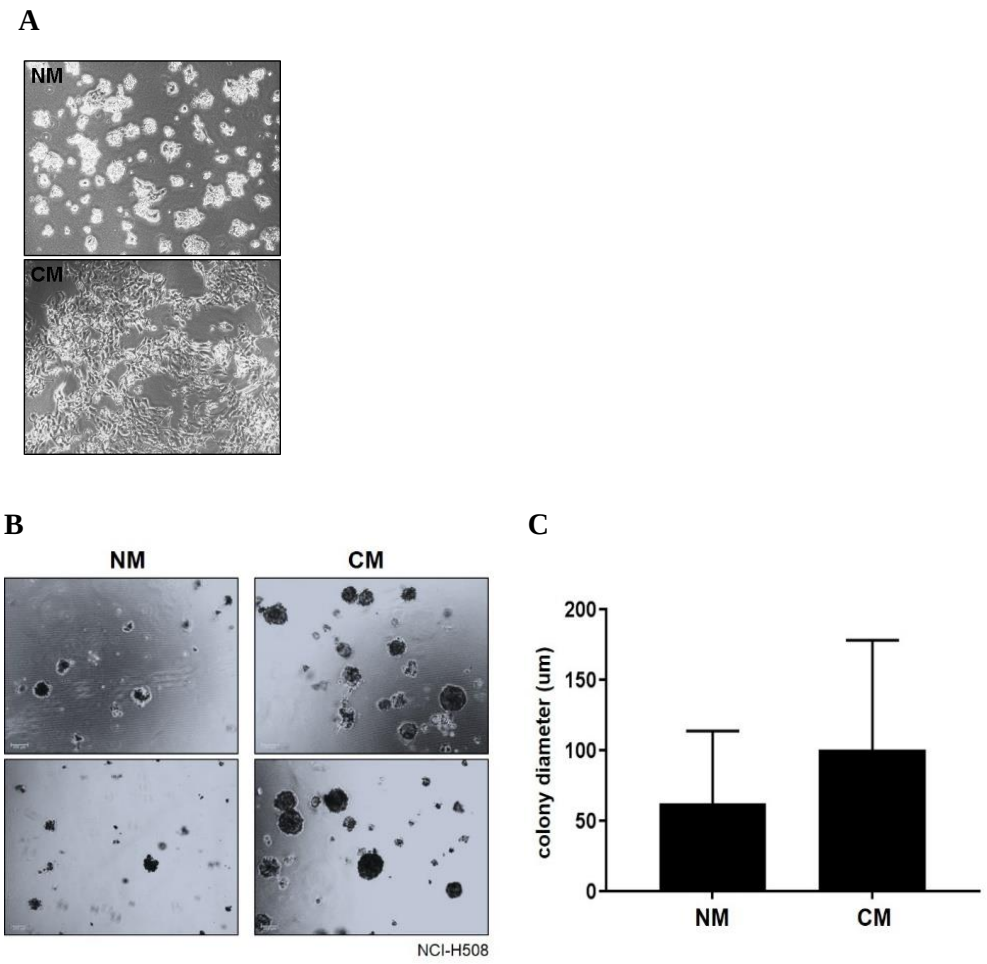

Figure 2. Conditioned medium from endogenously and exogenously expressing KRAS^{MT} cells affects the tumorigenesis in KRAS^{WT} cells. (A) NCI-H508^{WT} cells were treated with NM and CM for 48hrs and the images were observed by microscopy. **(B)** NCI-H508^{WT} cells were cultured in Matrigel for 3D culture. Each seeded cells were treated with NM and CM. Scale bars 100 μm. **(C)** Colony diameter was measured by microscopy.

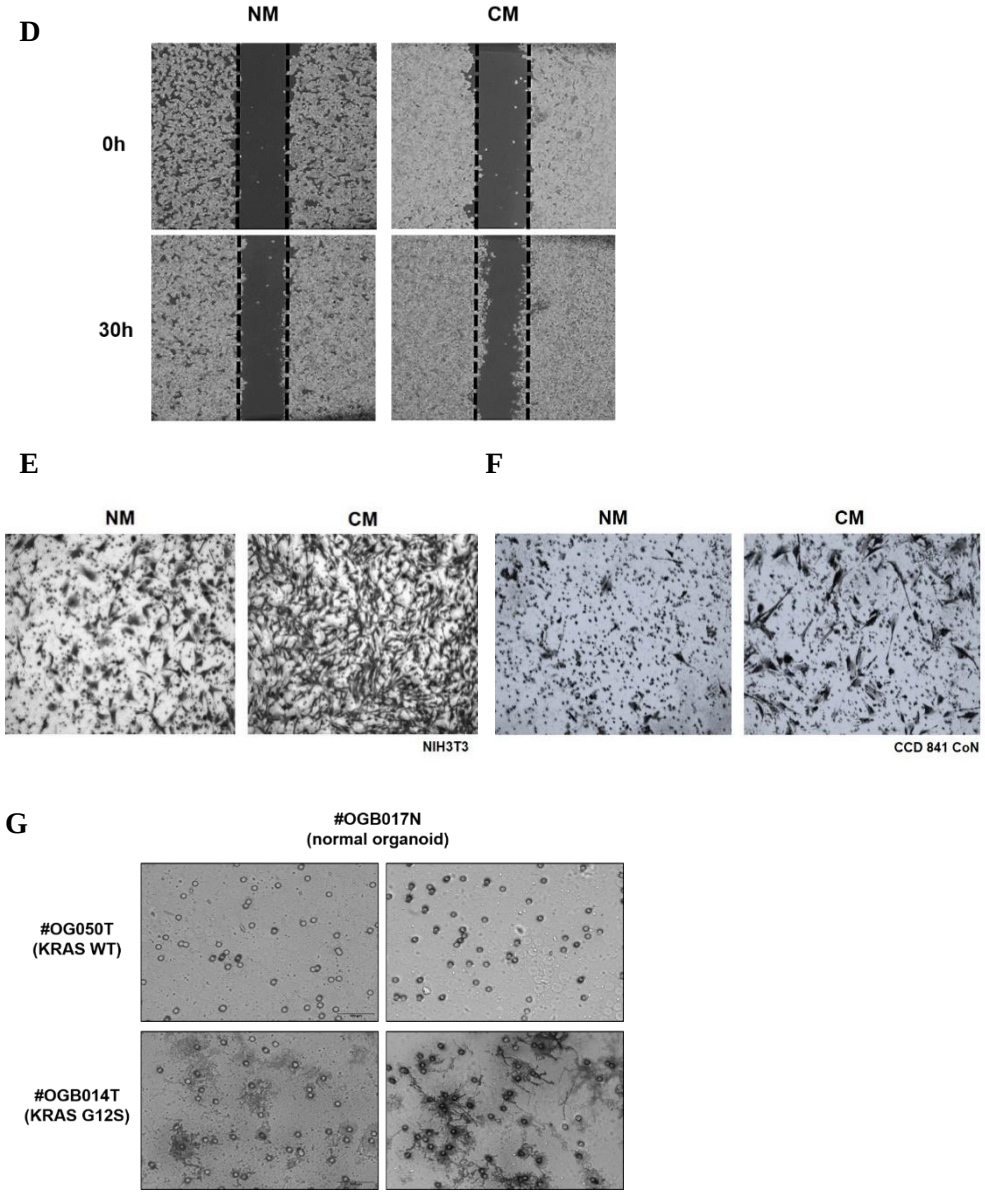

Figure 2. (D) Wound healing assay was conducted by using DiFi^{WT} cells and treated with NM and CM. cell motility was observed from 0hr and 30hrs. **(E)**

NIH3T3^{WT} cells were seeded in insert chamber with serum-free media and cultured in NM and CM treated plate. **(F)** CCD-841-CoN^{WT} cells were seeded in insert chamber with serum-free media and cultured in NM and CM treated plate. **(G)** Colorectal normal organoids^{WT} were seeded in insert chamber with serum-free media and cultured in NM from KRAS wild-type organoid and CM from KRAS-mutant-type organoid treated plate.

To directly observe the influence by KRAS mutation to tumorigenecity, I over-expressed KRAS G12V in NCI-H508^{WT} cells and harvested NM^{VEC} and CM^{G12V} from empty vector and KRASG12V transfected NCI-H508^{WT} cells, respectively (Figure 2H). NCI-H508^{WT} cells were cultured with NM^{VEC} and CM^{G12V} for 48hrs than I observed that cell morphology was changed when cultured with CM^{G12V} compared with NM (Figure 2I). I seeded NCI-H508^{WT} cells in Martrigel for three-dimensional culture and treated NM^{VEC} and CM^{G12V} to observe the influence of CM^{G12V} for tumorigenecity (Figure 2J and K). I observed that the colony diameter was significantly increased when CM^{G12V} was treated compared with NM^{VEC} treatment.

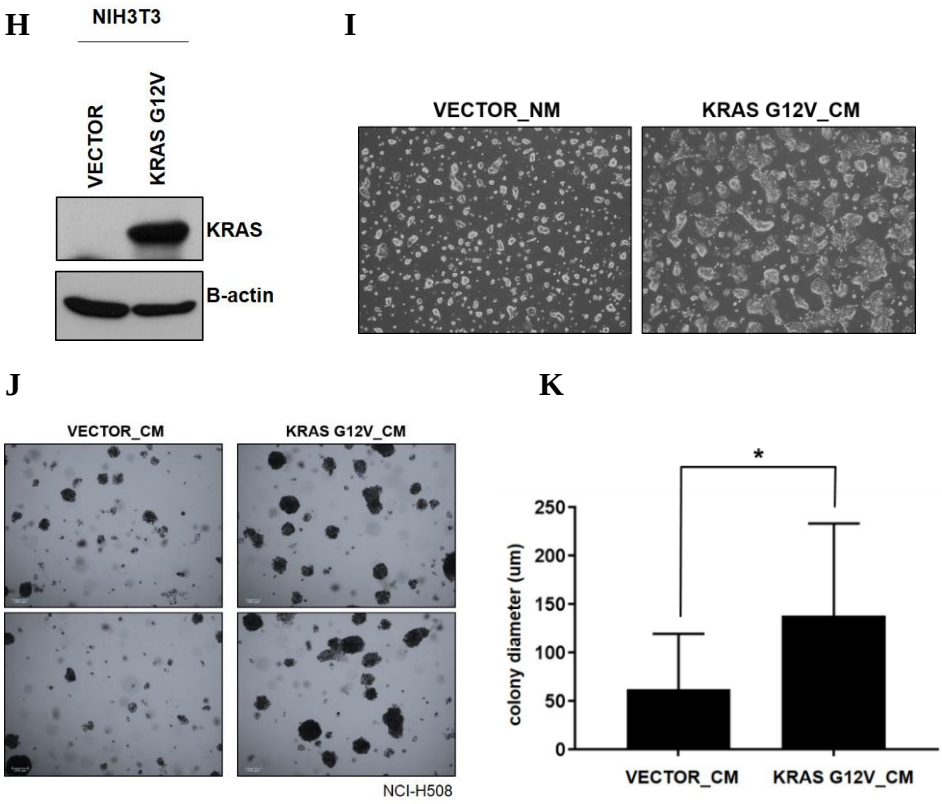

Figure 2. (H) Empty vector and $KRAS^{G12V}$ were transfected to $NIH3T3^{WT}$ cells and it was observed by western-blotting. **(I)** $NCI\text{-}H508^{WT}$ cells were treated with NM and CM from $NIH3T3^{VEC}$ cells and $NIH3T3^{G12V}$ cells, respectively, for 48hrs and the images were observed by microscopy. **(J)** $NCI\text{-}H508^{WT}$ cells were cultured in Matrigel for three-dimensional culture for 14 days and colony spheroid formation was observed after NM and CM from $NIH3T3^{VEC}$ cells and $NIH3T3^{G12V}$ cells, respectively. Scale bars 100 μm. **(K)** Colony diameter was measured by microscopy.

Conditioned medium from $KRAS^{MT}$ cells promotes the cetuximab resistance in $KRAS^{WT}$ cells

Next, I investigated that cetuximab which is a targeted drug for $KRAS^{WT}$ colorectal cancer patients was also influenced by CM in tumor microenvironment. To observe that $KRAS^{WT}$ cells are also influenced cetuximab resistance by surrounding $KRAS^{MT}$ cells through paracrine-signal, I investigated the relationship between CM and cetuximab response. First, I tested in vitro response of cetuximab as single agents, in colorectal cancer cell (NCI-H508, DiFi, HCT-116, colo-320, and SNU-C5) having different mutation in PIK3CA, EGFR, KRAS genes (Figure 3A). Cancer cells were treated with cetuximab at concentrations ranging from 0.1 to 100 μg/mL for 72hrs and I selected NCI-$H508^{WT}$ and $DiFi^{WT}$ cells, known as cetuximab sensitive and KRAS wild-type cells. To investigate whether CM affects response to the cetuximab, I treated cetuximab with NM and CM for 72hrs and observed CM led to cetuximab resistance to $KRAS^{WT}$ cells (Figure 3B and C). Furthermore, the effect of cetuximab was analyzed on colonogenic survival of 2D-grown by colony forming assay (Figure 3D) and I observed resistance to cetuximab when CM was treated compared with NM. Figure 3E showed to co-culture results. NCI-$H508^{WT}$ cells were co-cultured with HCT-116^{MT} and NCI-$H508^{WT}$ cells and treated with 100 μg/mL cetuximab for 48hrs. Immunofluorescent staining using a BrdU label confirmed that cetuximab inhibited cell proliferation when cultured

with $KRAS^{WT}$ cells, but it was protected from cetuximab when co-culture with $KRAS^{MT}$ cells.

These results suggested that CM from $KRAS^{MT}$ cells resulted in cetuximab resistance to $KRAS^{WT}$ cells.

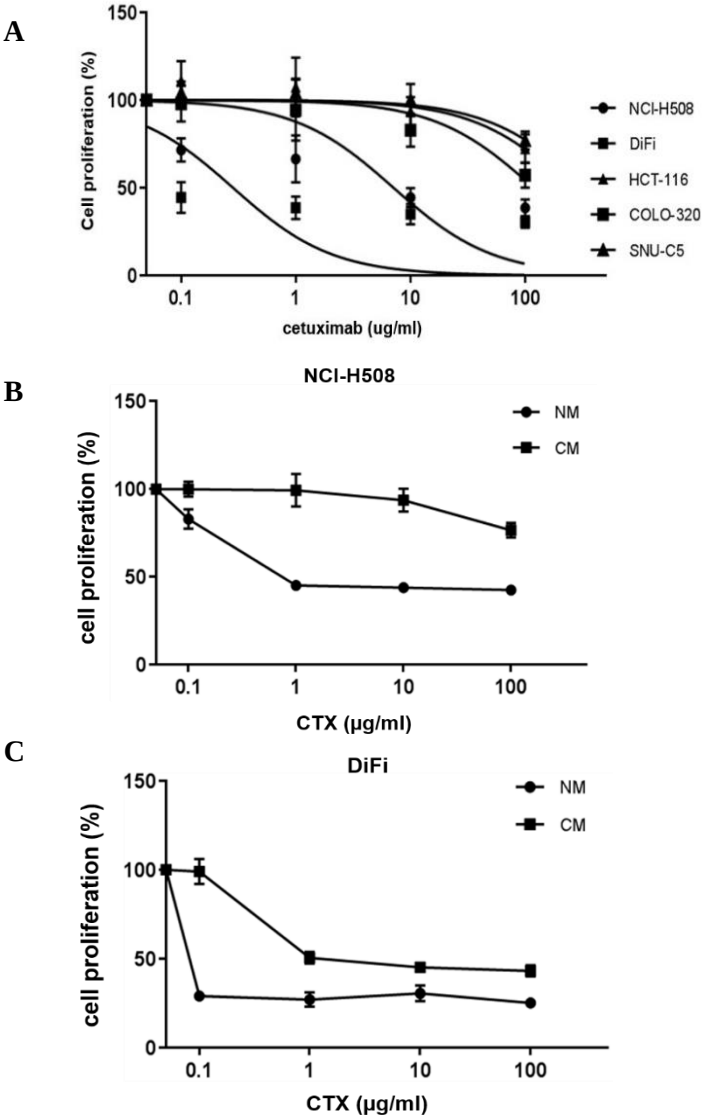

Figure 3. Conditioned medium from endogenously and exogenously expressing KRAS^{MT} cells affects the cetuximab resistance in KRAS^{WT} cells. (A) Percentage of survival of cells treated with increasing doses of cetuximab (0.1, 1, 10, and 100 μg/mL) for 72hrs was measured by the MTT assay. Data represent

means ± SD of three independent experiments. **(B)** Percentage of survival of NCI-H508^{WT} cells treated with increasing doses of cetuximab (0.1, 1, 10, and 100 µg/mL), in NM or CM, as measured by the MTT assay. Data represent means ± SD of three independent experiments. **(C)** Percentage of survival of DiFi^{WT} cells treated with increasing doses of cetuximab (0.1, 1, 10, and 100 µg/mL), in NM or CM, as measured by the MTT assay. Data represent means ± SD of three independent experiments.

D

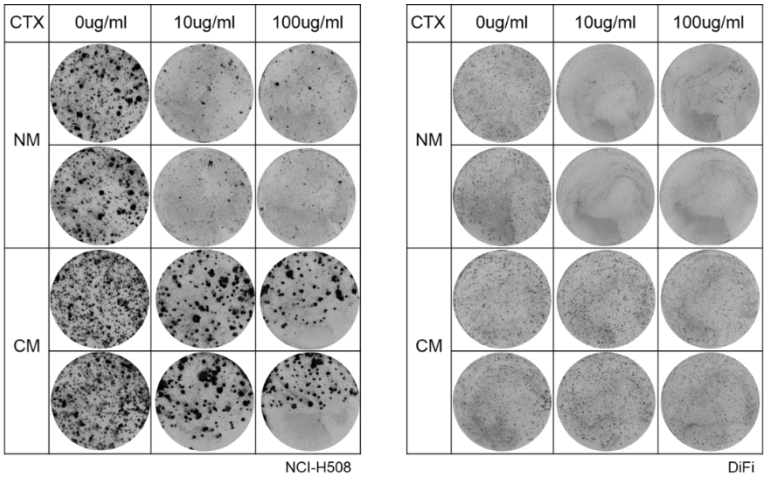

E

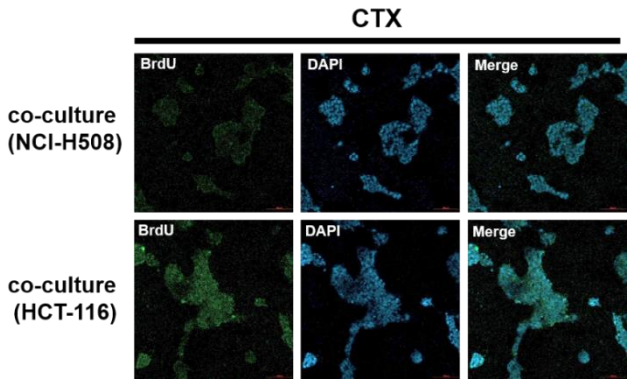

Figure 3. (D) Clonogenic assay images of NCI-H508^{WT} and DiFi^{WT} cells after cetuximab (10 and 100 μg/mL) treatment with NM and CM on day 14. **(E)** NCI-H508^{WT} cells were co-cultured with NCI-H508^{WT} cells and HCT-116^{MT} cells. After 24hrs, cetuximab (100 μg/mL) was treated for 48hrs and proliferated cells were observed by BrdU assay.

To directly observe the influence of cetuximab resistance by KRAS mutation, I also investigated the relationship between exogenously over-expressed mutant KRAS derived CM and cetuximab resistance in $KRAS^{WT}$ cells (Figure 3F). Although NCI-$H508^{WT}$ cells are not harboring KRAS mutation, cetuximab resistance was occurred when CM^{G12V} treated (Figure 3G). I conducted three-dimensional culture in which NM^{VEC} and CM^{G12V} treated with cetuximab in NCI-$H508^{WT}$ cells and after a 2-weeks incubation period, spheroid was documented by microscopy (Figure 3H). As expected, NCI-$H508^{WT}$ cells which treated cetuximab with CM^{G12V} were not influenced by cetuximab compared with NM^{VEC} treated case. In addition, NCI-$H508^{WT}$ cells were co-cultured with NCI-$H508^{VEC}$ and NCI-$H508^{G12V}$ cells and treated with 100 μg/mL cetuximab for 48hrs. Immunofluorescent staining using a BrdU label confirmed that cetuximab inhibited cell proliferation when cultured with $KRAS^{WT}$ cells, but it was protected from cetuximab when co-culture with NCI-$H508^{G12V}$ cells (Figure 3I).

These results suggested that conditioned media containing secretion factors from mutant KRAS expressed cells endogenously and exogenously effected tumor progressions and cetuximab resistance in surround $KRAS^{WT}$ cells.

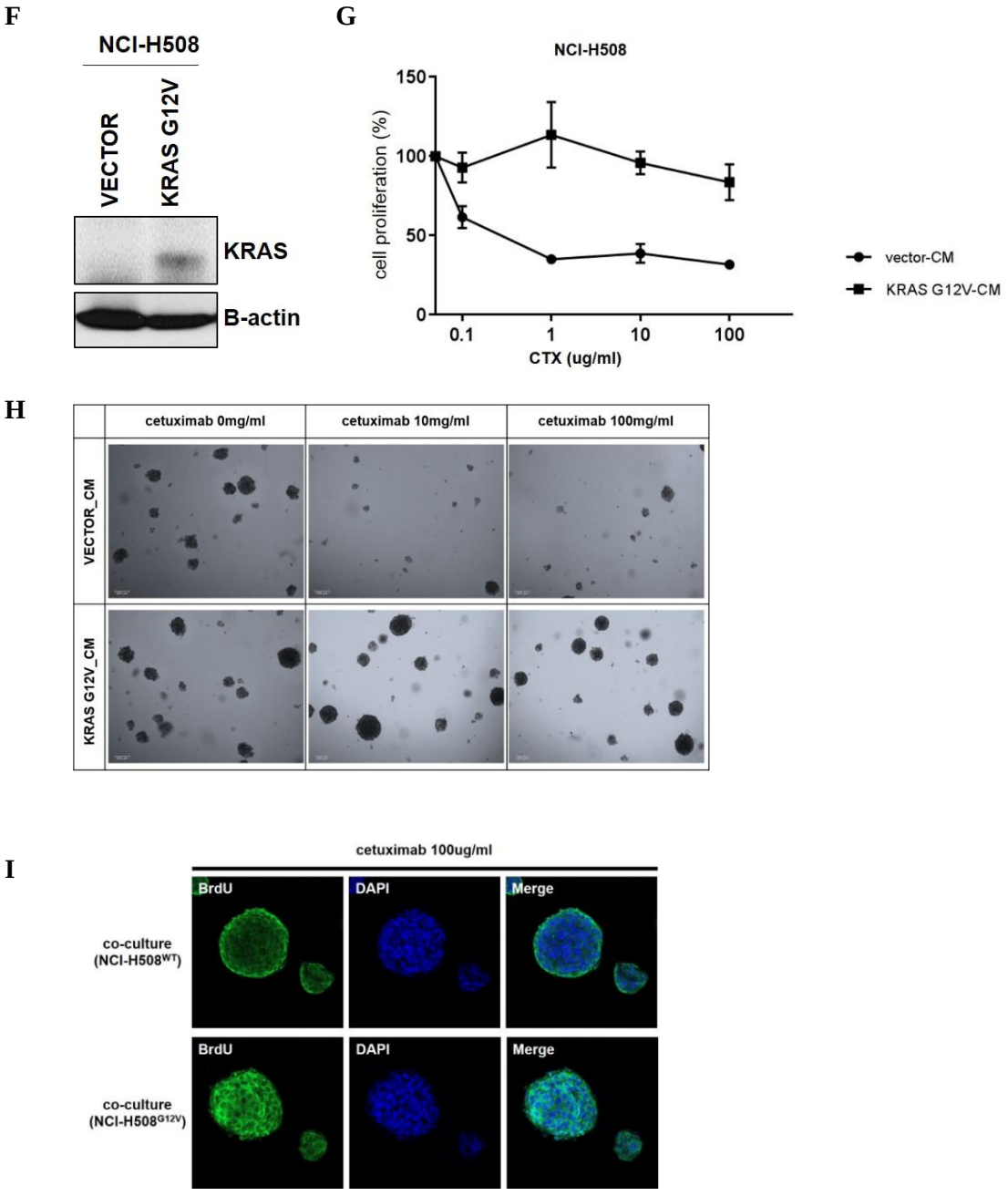

Figure 3. (F) Empty vector and mutant KRAS G12V were transfected to NCI-

H508^{WT} cells and it was observed by western-blotting. **(G)** Percentage of survival of NCI-H508^{WT} cells was measured by the MTT assay after treated with increasing doses of cetuximab (0.1-100 μg/mL) with NM and CM from NCI-H508^{VEC} cells and NCI-H508^{G12V} cells, respectively. Data represent means ± SD of three independent experiments. **(H)** NCI-H508^{WT} cells were cultured in Matrigel for three-dimensional culture for 14 days and colony spheroid formation was observed after cetuximab (10 and 100 μg/mL) treatment with NM and CM from NCI-H508^{VEC} cells and NCI-H508^{G12V} cells, respectively. Scale bars 100 μm. **(I)** NCI-H508^{WT} cells were co-cultured with NCI-H508^{VEC} cells and NCI-H508^{G12V} cells. After 24hrs, cetuximab (100 μg/mL) was treated for 48hrs and proliferated cells were observed by BrdU assay.

Identification of secretion factor from $KRAS^{MT}$ cells in conditioned media

The experiments above suggest that protective paracrine interactions could be mediated by cytokines in the CM. To identify specific tumorigenic factors present in CM from $KRAS^{MT}$ cells, I conducted proteomics analysis of $KRAS^{WT}$ cells (SNU-C5) and $KRAS^{MT}$ cells (HCT-15 and LS174T) to check the differential protein expression among these cell lines. And I classified the genes by their localization. Total 6191 genes were detected (Figure 4A). To focus my studies on those factors with clear potential for paracrine effects on tumor cells, I evaluated genes with at least 2-fold elevated expression in $KRAS^{MT}$ cells that both encoding extracellular proteins (Figure 4B). Since, MIF gene is reported to be associated in tumorigenecity and metastasis particularly in colorectal cancer [24], I have been studied on MIF gene. First, I checked the protein expression of 5 $KRAS^{WT}$ and 6 $KRAS^{MT}$ cells by western-blotting (Figure 4C), MIF expression was higher in $KRAS^{MT}$ cells compared with $KRAS^{WT}$ cells.

A

Location	The number of gene
Extracelluar space	285
Plasma membrane	643
Cytoplasm	2849
Nucleus	1741
other	677
Total	**6191**

C

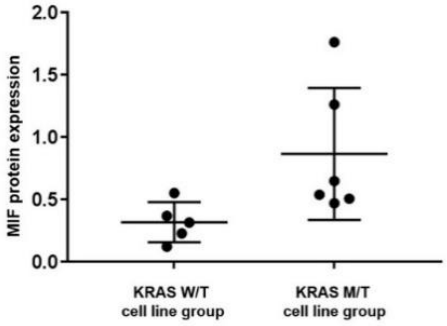

B

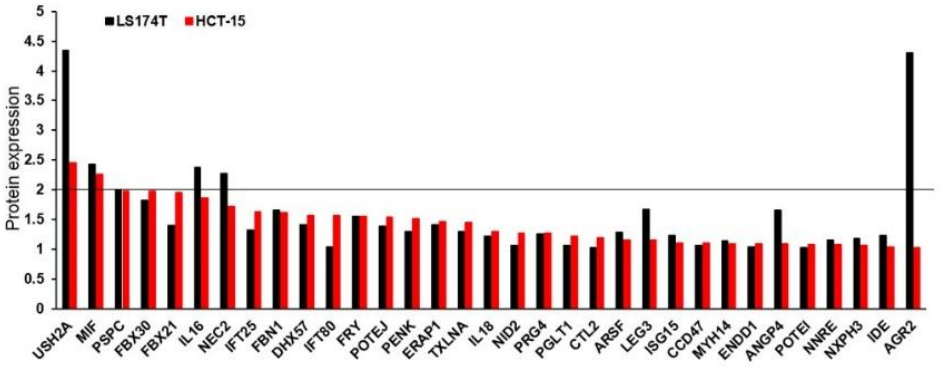

Figure 4. MIF expression and secretion is increased in KRAS^{MT} colorectal cancer cells and patients. (A) Proteomics analysis of KRAS^{WT} cells (SNU-C5) and KRAS^{MT} cells (HCT-15 and LS174T) was conducted to check the differential protein expression among these cell lines. And the genes were classified by their localization. **(B)** Genes were evaluated with at least 2-fold elevated expression in KRAS^{MT} cells that both encoding extracellular proteins. **(C)** Protein expression of KRAS^{WT} and KRAS^{MT} cells was checked by western-blotting.

In addition, mRNA expression was also shown high expression of MIF in $KRAS^{MT}$ cells (Figure 4D). MIF mRNA expression in 15 $KRAS^{WT}$ and $KRAS^{MT}$ colorectal cancer patient tissues was analyzed by using RNA-sequencing data (Figure 4E). I observed that MIF expression was also higher in the $KRAS^{MT}$ patients compared with $KRAS^{WT}$ patients. The experiments above suggest that protective paracrine interactions could be mediated by MIF in the CM. To identify secreted MIF level, conditioned media by $KRAS^{WT}$ and $KRAS^{MT}$ from each of cell groups were investigated using human MIF ELISA assay (Figure 4F). The presence of the MIF was measured after 48hrs of incubation. CM showed significantly higher concentration of MIF compared with $KRAS^{WT}$ cells. Moreover, MIF serum levels of colorectal cancer patients were measured and MIF secretion was elevated in $KRAS^{MT}$ patient group compared with $KRAS^{WT}$ patient group (Figure 4G). Therefore, these results suggested that MIF expression was higher in the $KRAS^{MT}$ cells and also highly secreted from $KRAS^{MT}$ cells and patients, compared to $KRAS^{WT}$ group.

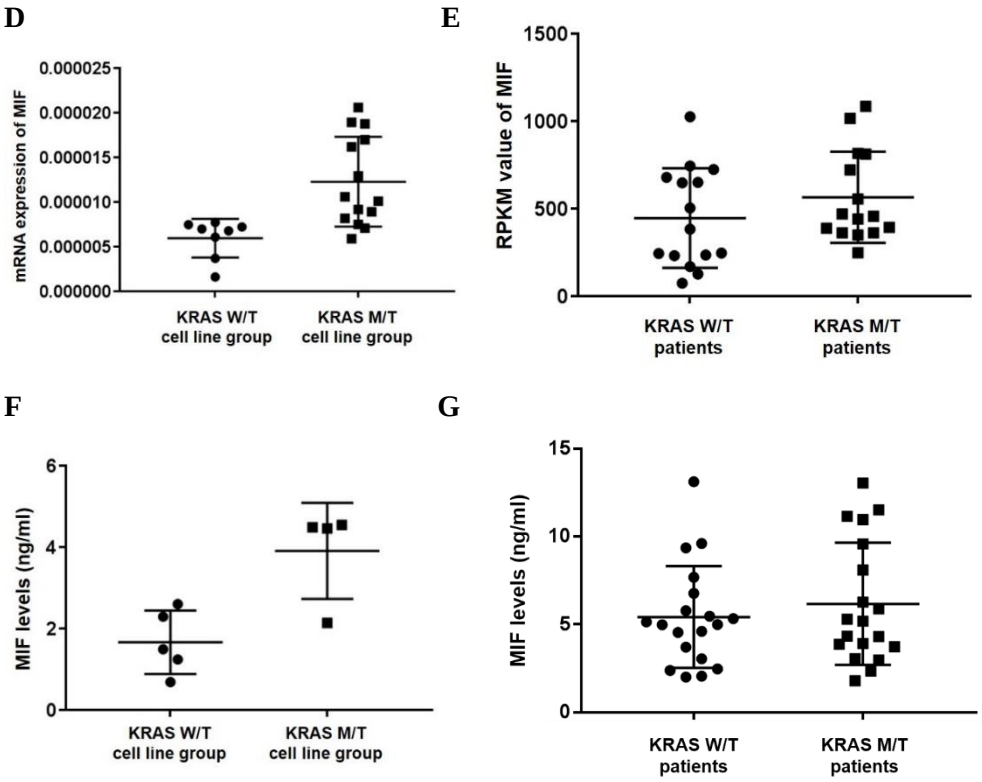

Figure 4. (D) mRNA expression of $KRAS^{WT}$ and $KRAS^{MT}$ cells were checked by qRT-PCR. **(E)** RPKM value of $KRAS^{WT}$ and $KRAS^{MT}$ patient samples was analyzed in RNA sequencing data. **(F)** MIF levels in $KRAS^{WT}$ and ^{MT} cells were measured by human MIF ELISA. **(G)** MIF levels in serum of 19 $KRAS^{WT}$ and 20 $KRAS^{MT}$ patients were measured by human MIF ELISA. Data represent means ± SD of two independent experiments, $P<0.5$.

To prove cetuximab resistance by MIF in CM, I treated 30μM MIF inhibitor 4-IPP with CM in NCI-H508^{WT} cells (Figure 5A). The cetuximab resistance by MIF containing CM was restored by treating MIF inhibitor 4-IPP compared with non-treated inhibitor. Although, activation of AKT signal was blocked when cetuximab treated with NM (lane 2), it was not blocked by cetuximab when treated with CM (lane 4), blocking EGFR signal in both. However, AKT signal was blocked with treatment of 4-IPP (lane 5 and 6) without blockage of EGFR (Figure 5B). Furthermore, I knocked down CD74 known as MIF receptor in NCI-H508^{WT} cells by using siRNA system and it could not result in cetuximab resistance when cetuximab was treated with CM (Figure 5A and B).These results provided direct evidence that paracrine-MIF leads to cetuximab resistance through CD74-AKT signaling activation bypass from EGFR signaling.

A

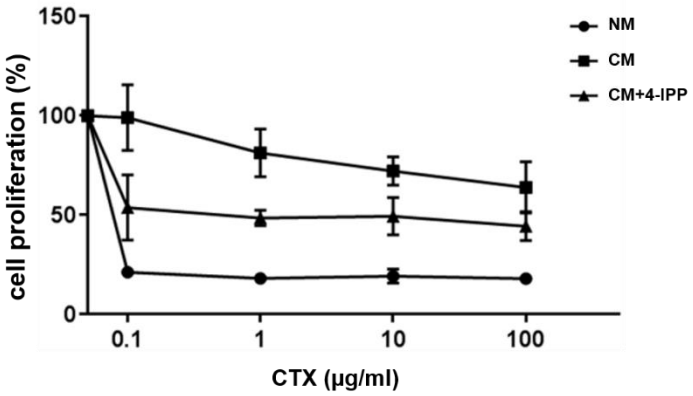

B

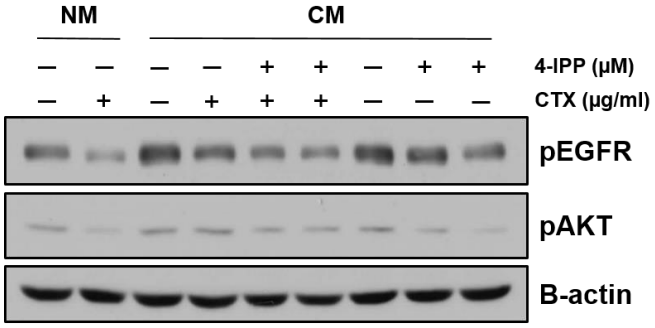

Figure 5. Influence of MIF on the cetuximab resistance through CD74 receptor in KRAS^{WT} cell lines. (A) Increasing doses of cetuximab (0.1, 1, 10, and 100 μg/mL) was treated to NCI-H508^{WT} cells with NM, CM, and CM with 20 uM 4-IPP, respectively. Percentage of survival was measured by MTT assay. Data represent means ± SD of three independent experiments. **(B)** Cetuximab (0, 10, and 100 μg/mL) was treated in NCI-H508^{WT} cells with CM, NM, and CM with 20 uM 4-IPP and AKT signaling was observed by western-blotting.

C

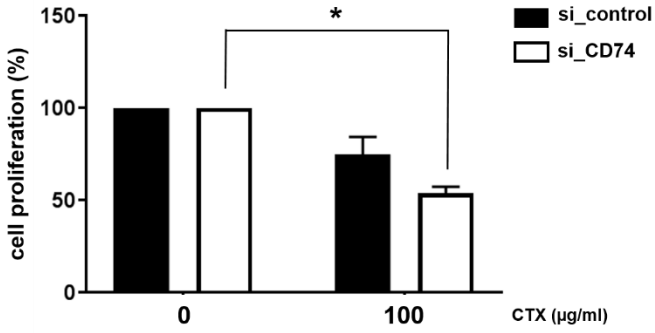

D

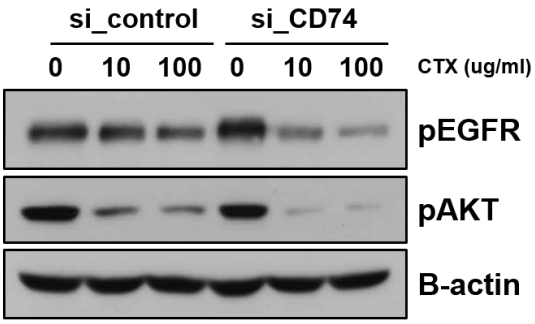

Figure 5. (C) NCI-H508^{WT} cells were treated with 100 μg/mL cetuximab after CD74 knock down. Percentage of survival of NCI-H508^{WT} cells was measured by the MTT assay after 72hrs. Data represent means ± SD of three independent experiments. **(D)** Cetuximab (0, 10, and 100 μg/mL) was treated in CD74 knocked out NCI-H508^{WT} cells and control. AKT signaling was observed by western-blotting.

MIF promotes cetuximab resistance to KRAS^{WT} cells by paracrine-signaling and over-expression

The preceding experiments suggested that paracrine-acting oncogenic KRAS-induced MIF may influence the response of tumor cells to cetuximab resistance. MIF directly stimulates PI3K/AKT signaling [25]. To determine the contribution of oncogenic KRAS-induced MIF to cetuximab resistance, SNU-C5^{WT} cells were treated with human recombinant MIF (rhMIF) at a concentration of 50 and 100 ng/mL exogenously (Figure 6A) and AKT phosphorylation evaluated. rhMIF led to increase of endogenous AKT and S6 phosphorylation with a stimulation observed at 30 to 180min. DiFi^{WT} cells treated to rhMIF consistently showed attenuation of cetuximab induced cytotoxicity at a 100 ng/mL rhMIF concentrations after 72hrs (Figure 6B). To investigate whether AKT activation by MIF led to cetuxmab resistance, I applied cetuximab with rhMIF in DiFi^{WT} cells (Figure 6C). Cetuximab completely suppressed the phosphorylation of EGFR in both treated and non-treated rhMIF, however, AKT signaling was not blocked by cetuximab when rhMIF was treated with cetuximab.

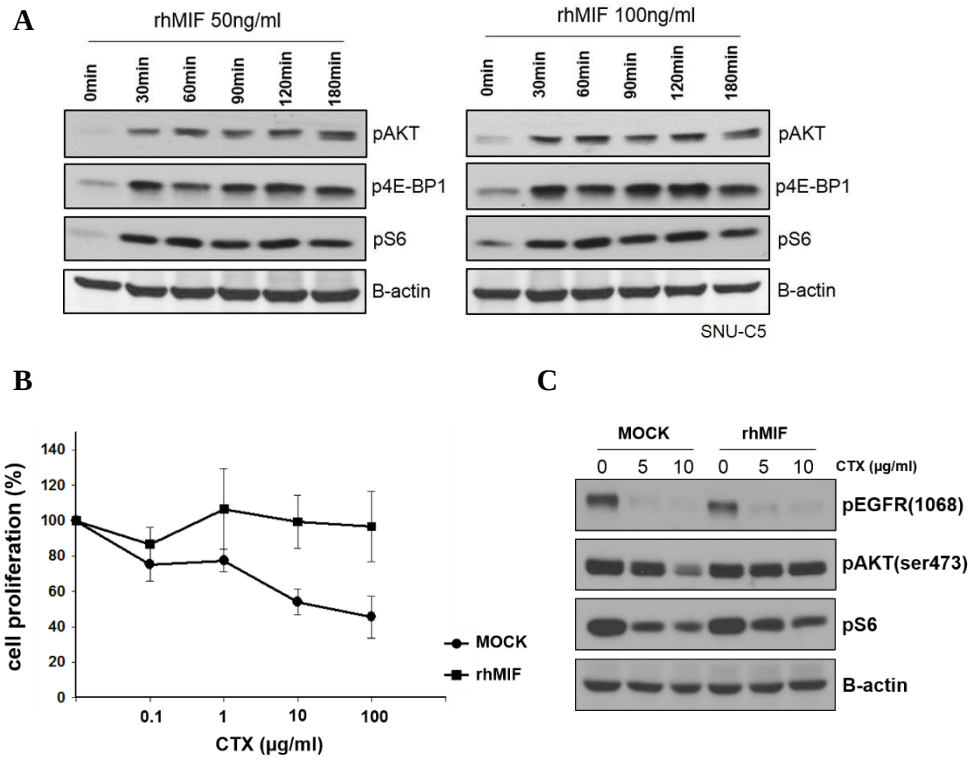

Figure 6. Paracrine MIF effects on cetuximab resistance through AKT signaling pathway. (A) Human recombinant MIF 50 and 100 (ng/mL) was treated in SNU-C5^{WT} cells in time dependently and AKT signaling was observed by western-blotting. **(B)** DiFi^{WT} cells were treated with increasing doses of cetuximab (0.1, 1, 10, and 100 μg/mL) with DW and rhMIF. Percentage of survival of DiFi^{WT} cells was measured by the MTT assay after 72hrs. Data represent means ± SD of three independent experiments. **(C)** Cetuximab (0, 10, and 100 μg/mL) was treated in DiFi^{WT} cells with rhMIF and AKT signaling was observed by western-blotting.

Next, I over-expressed MIF gene and stably transfected in NCI-H508^{WT} cells. NCI-H508^{MIF} increased the viability of exposed to cetuximab concentration ranging between 0.1 to 100 μg/mL compared with NCI-H508^{VEC} (Figure 6D). EGFR signaling was also inhibited by cetuximab in NCI-H508^{VEC} and NCI-H508^{MIF}. However, when MIF was over-expressed AKT signaling was not blocked in NCI-H508^{MIF} cells and it was observed by western-blotting (Figure 6E). I addition to, it was also observed by BrdU assay (Figure 6F).

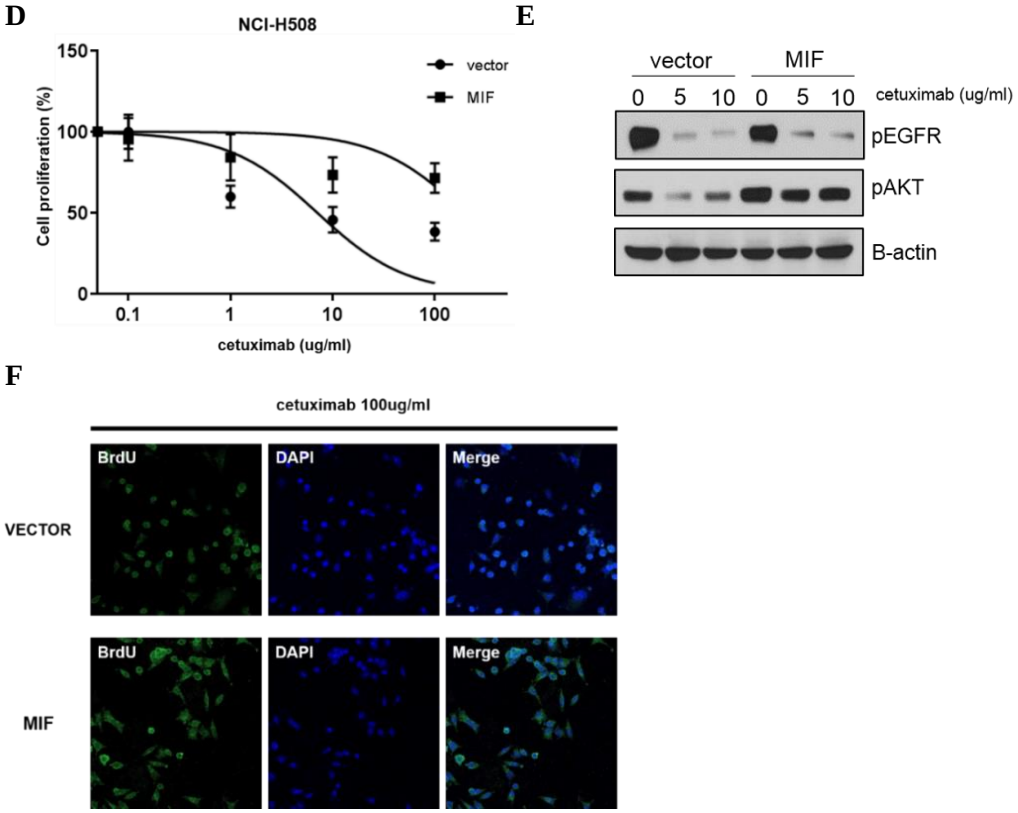

Figure 6. (D) Percentage of survival of NCI-H508^{VEC} and NCI-H508^{MIF} cells was measured by the MTT assay after treated with increasing doses of cetuximab (0.1, 1, 10, and 100 μg/mL). Data represent means ± SD of three independent experiments. **(E)** Cetuximab (0, 10, and 100 μg/mL) was treated in empty vector and MIF over-expressed NCI-H508 cells with rhMIF and AKT signaling was observed by western-blotting. **(F)** NCI-H508^{WT} and NCI-H508^{MIF} cells were treated with cetuximab (100 μg/mL) for 48hrs and proliferated cells were observed by BrdU assay.

I then wanted to investigate above data on CM, weather it was HCT-116^{MT} cell line specific effects or not, I harvested conditioned media from DiFi^{WT}, SNU-70^{WT}, HT-29^{WT}, and HCT-116^{MT} cells. As expected, cell viability was not inhibited following treatment of cetuximab with CM in only treated CM from HCT-116^{MT} cells (Figure 6G). After that, I used CRISPR-based method to genetically disrupt MIF in HCT-116^{MT} cells. Western-blotting analysis of HCT-116^{MT} cells expressing sgMIF, using anti-MIF antibody showed the total absence of endogenous MIF protein (Figure 6H) and mRNA expression was decreased (Figure 6I). Then I checked secreted MIF level from HCT-116^{MT} cells by ELISA (Figure 6J). Although HCT-116^{MT} cells are carrying KRAS mutation, when MIF gene was knocked out, MIF secretion was decreased. To evaluate the influence of MIF on the cetuximab resistance, I treated cetuximab with CM from HCT-116^{MT} and HCT-116$^{MT/MIF\ KO}$ (Figure 6K). When MIF was knocked out in HCT-116^{MT} cells, I observed that CM treatment from HCT-116$^{MT/MIF\ KO}$ cells was not shown the effects of cetuximab resistance compared CM treatment from HCT-116^{MT} cells although the CM was harvested from KRAS mutant cells. These findings reveal that inhibition of this paracrine MIF contributed to restore cetuximab resistance by MIF in KRAS^{WT} colorectal cancer cells.

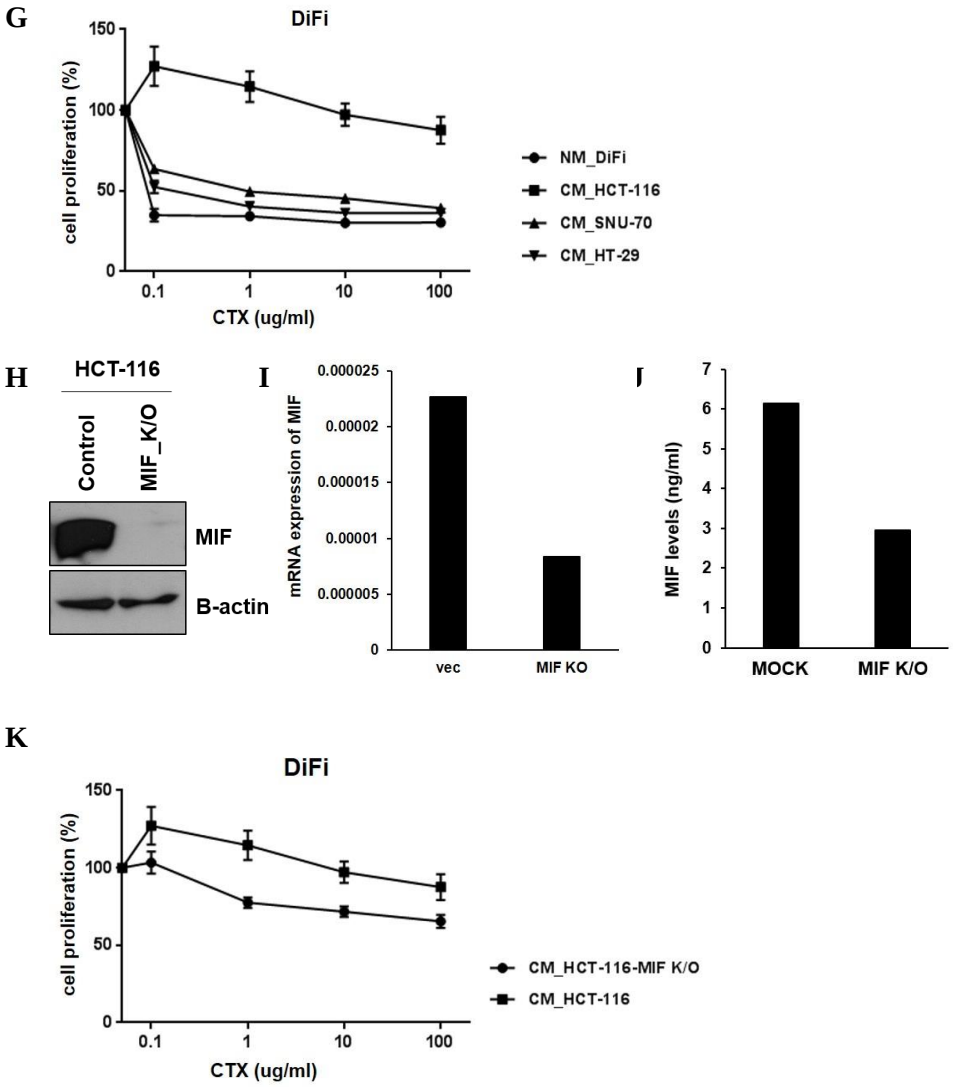

Figure 6. (G) DiFi^{WT} cells were treated with increasing doses of cetuximab (0.1, 1, 10, and 100 μg/mL) with NM (DiFi^{WT} cells) and CM (HCT-116^{MT} cells, SNU-70^{WT} cells, and HT-29^{WT} cells). Percentage of survival was measured by MTT assay. Data represent means ± SD of three independent experiments. **(H)** MIF was

knocked out by CRISPR/Cas9 system in HCT-116^{MT} cells and it was confirmed by western-blotting. **(I)** mRNA expression of MIF was observed by qRT-PCR. **(J)** Secreted MIF levels were measured by human MIF ELISA assay. **(K)** Percentage of survival of DiFi^{WT} cells was measured by the MTT assay after treated with increasing doses of cetuximab (0.1, 1, 10, and 100 μg/mL) with NM and CM from HCT-116^{MT} cells and HCT-116$^{MIF\ K/O}$ cells, respectively. Data represent means ± SD of three independent experiments.

MIF transcription is directly regulated through NF-kB activation by following KRAS mutation

To gain insight into the mechanisms how oncogenic KRAS-derived MIF is regulated, I over-expressed KRAS G12V in NIH3T3^{WT} cells and discovered MIF expression was increased when mutant KRAS was over-expressed (Figure 7A and B). Furthermore, secretion level of MIF was measured in KRAS G12A, G12C, G12D, G12S, G12V, G13D, and Q61L over-expressed cells by ELISA (Figure 7C). MIF was highly secreted when diverse KRAS mutant form were over-expressed. To investigate that MIF transcription is regulated by KRAS mutation status, I examined the effects of KRAS mutation on MIF activity in NIH3T3^{WT} cells (Figure 7D). NIH3T3^{WT} cells were transiently transfected with MIF-Luc reporter plasmid, and reporter activity was found to be regulated by KRAS mutant amounts indirectly. To figure out the direct mechanism between oncogenic KRAS and MIF, I found candidates of transcription factors targeting MIF. Therefore, I investigated whether the introduction NF-kB which activated by mutant KRAS regulates MIF transcriptional activity. NF-kB activation is related to the nuclear translocation. I analyzed the distribution of NF-kB factors in the cytoplasm and nucleus by western blot analysis after KRAS G12V transfection in NCI-H508^{WT} and DiFi^{WT} cells (Figure 7E). Compared with the control, NF-kB was located in the nucleus when KRAS G12V was over-expressed, suggesting that the oncogenic KRAS activates

NF-kB. Next, mRNA expression of MIF was observed when NF-kB was over-expressed and knocked down by siRNA (Figures 7F and G) and MIF expression was regulated by NF-kB expression. Moreover, MIF transcription was regulated by NF-kB activation and it was observed by luciferase assay (Figure 7H).

These results indicate that oncogenic KRAS regulates MIF transcriptional activity through regulation of NF-kB transcription factors.

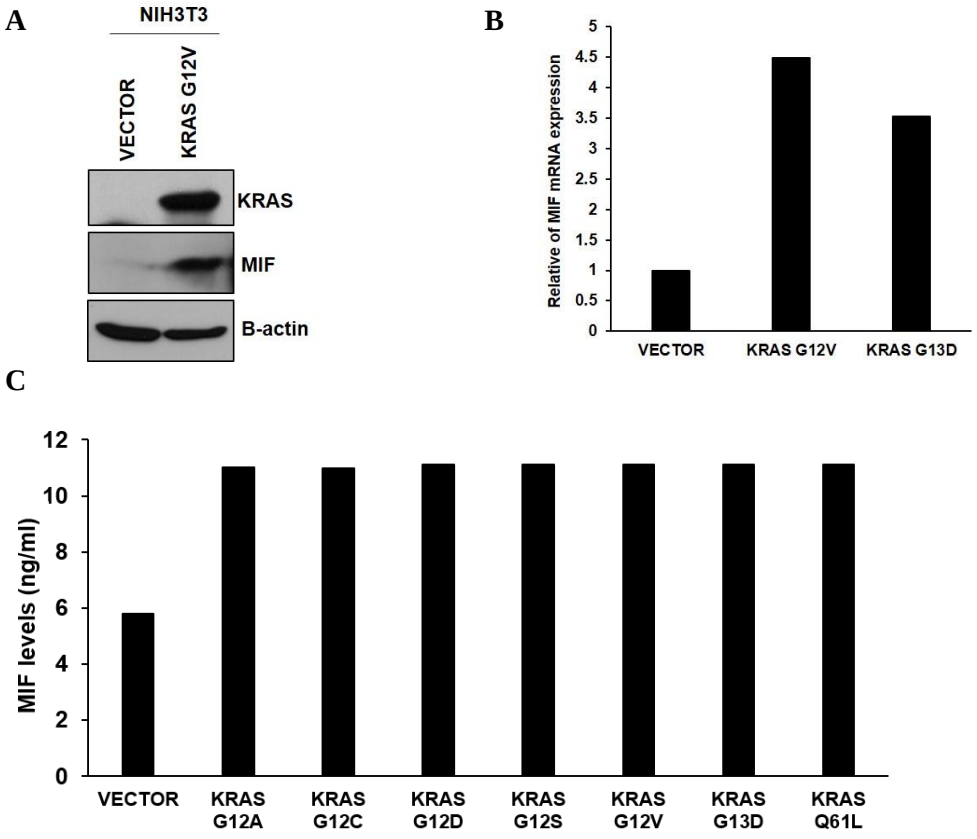

Figure 7. Oncogenic KRAS regulates MIF transcription and secretion through NF-kB. (A) Empty vector and KRAS G12V were transfected to NIH3T3^{WT} cells. Protein expression of KRAS and MIF was observed by western-blotting. **(B)** Empty vector and mutant KRAS (G12V and G13D) were transfected to NIH3T3^{WT} cells. mRNA expression of MIF was observed by qRT-PCR. **(C)** Secreted MIF levels were measured in KRAS G12A, G12C, G12D, G12S, G12V, G13D, and Q61L over-expressed cells by human MIF ELISA.

D

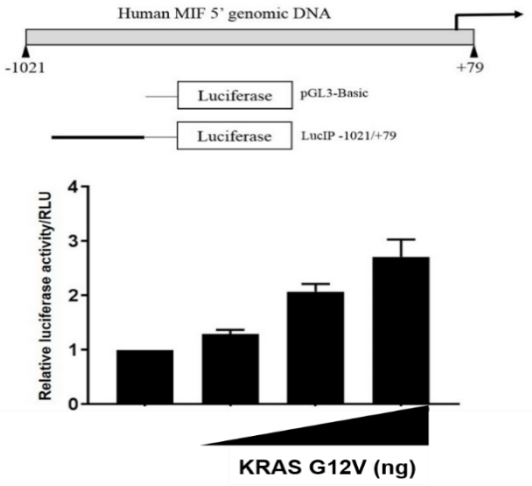

E

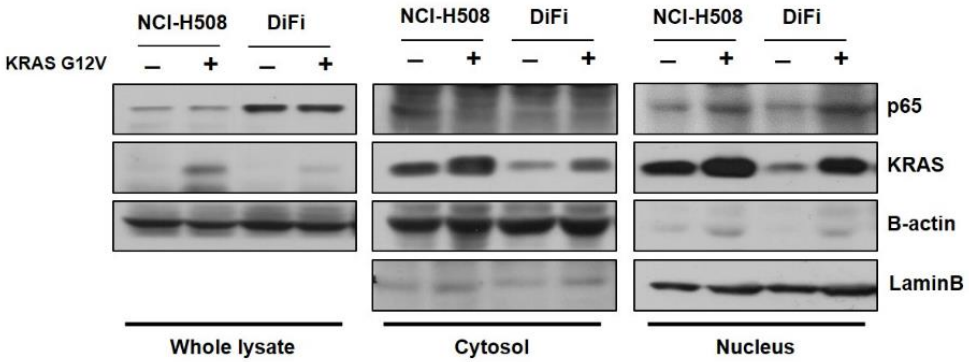

Figure 7. (D) Luciferase assay was conducted to measure MIF transcriptional levels with concentration (0, 100, 400, and 500 ng) of KRAS G12V dependently. Data represent means ± SD of three independent experiments. **(E)** Empty vector and KRAS G12V were transfected to NCI-H508^{WT} and DiFi^{WT} cells. The nuclear and cytosolic proteins were prepared for Western blot analysis. Lamin B and actin were used as internal controls for the nuclear and cytosolic fractions, respectively.

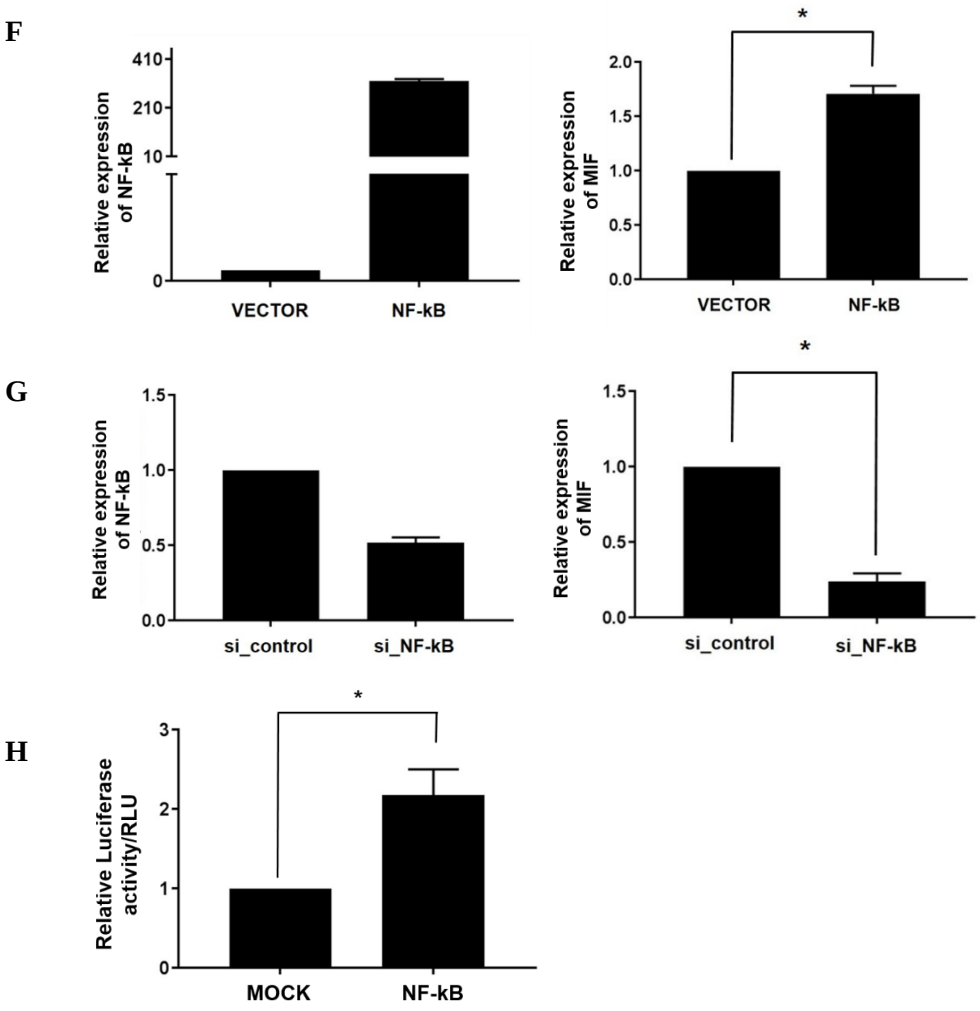

Figure 7. (F) Empty vector and NF-kB were transfected to DiFi^{WT} cells. mRNA expression of MIF was observed by qRT-PCR. **(G)** si_control and si_NF-kB were transfected to HCT-116^{MT} cells. mRNA expression of MIF was observed by qRT-PCR. **(H)** Luciferase assay was conducted to measure MIF transcriptional levels by NF-kB activation. Data represent means ± SD of three independent experiments.

Relation between MIF and cetuximab acquired resistance in colorectal cancer cells

I observed that secreted MIF from $KRAS^{MT}$ cells influenced to tumorigenesis and cetuximab resistance in surround of $KRAS^{WT}$ cells. I investigated that MIF could be use as a predictive biomarker to cetuximab resistance when cetuximab acquired resistance was occurred. I established cetuximab acquired resistant cell lines by using NCI-$H508^{WT}$ cells (Figure 8A). As seen in Figure 8B, colony formation ability of NCI-H508_CR^{Q61L} cells were not inhibited by cetuximab treatment compared with NCI-$H508^{WT}$ cells. Although the parental cells were wild-type for KRAS, resistant derivatives acquired KRAS Q61L mutation (Figure 8C).

A

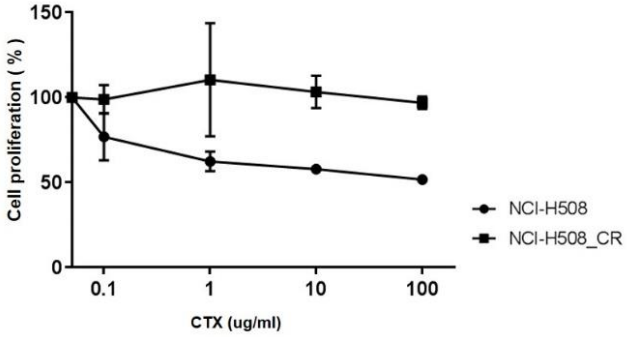

B

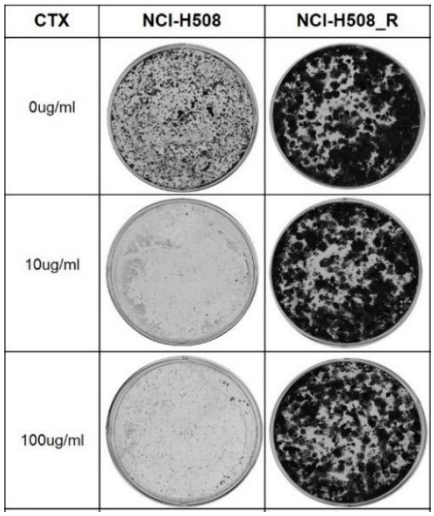

C

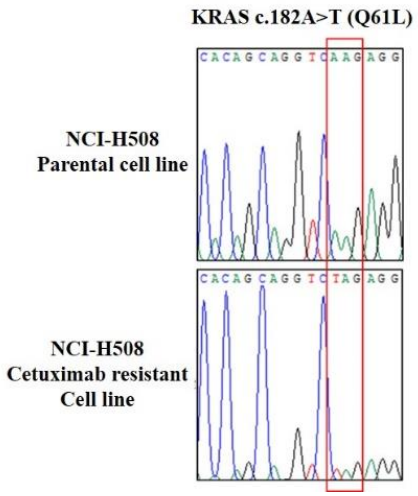

Figure 8. KRAS mutation-induced MIF mediated acquired resistance to cetuximab in NCI-H508^{WT} cells. (A) Cetuximab acquired resistant cells were produced by using NCI-H508^{WT} cells. Parental and NCI-H508_CR were produced by using NCI-H508^{WT} cells. Parental and NCI-H508_CR cells were treated for

72hrs with increasing concentrations of cetuximab. Cell viability was assayed by the MTT assay. Data points represent means ± SD of three independent experiments. **(B)** Colony formation assay was conducted with NCI-H508^{WT} and NCI-H508_CR^{Q61L} cells. NCI-H508^{WT} cells were treated with increasing dose of cetuximab (left line). NCI-H508_CR^{Q61L} cells were treated with increasing dose of cetuximab (right line). **(C)** Sanger sequencing of KRAS codon 61 in parental and NCI-H508_CR cells was conducted.

Since, MIF was highly secreted in KRAS Q61L over-expressing cells (Figure 7C), I measured secreted MIF levels. Secreted MIF level was increased in NCI-H508_CR^{Q61L} cells (Figure 8D). In the NCI-H508_CR^{Q61L} cells, I observed MIF expression and AKT phosphorylation was increased and MIF expression was also increased when cetuximab was treated (Figure 8E). Although, NCI-H508_CR^{Q61L} acquired KRAS Q61L mutation, resistance to cetuximab was relieved when 4-IPP was treated (Figure 8F). In western-blotting, AKT signaling was not blocked by cetuximab, however, it was blocked when 4-IPP combined treatment with cetuximab in NCI-H508_CR^{Q61L} cells (Figure 8G). Taken together, these results showed that cetuximab acquired resistant cells were acquired KRAS Q61L mutation and it led to elevation of MIF expression and secretion. My results demonstrating the secreted MIF in KRAS mutant-type cells raised question of whether MIF has the potential to serve as a predictive biomarker. This effect was demonstrated in KRAS wild-type patient serum samples who received cetuximab (Figure 9). I measured secreted MIF level of base line serum samples which patients who occurred disease progression (PD) and those who did not occur disease progression (non-PD). The secreted MIF level was high in the patients who occured disease progression (PD).

These results suggested that MIF may be a promising predictive biomarker for the cetuximab resistance of KRAS wild-type colorectal cancer patients.

D

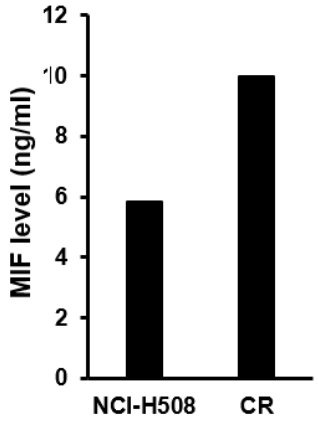

E

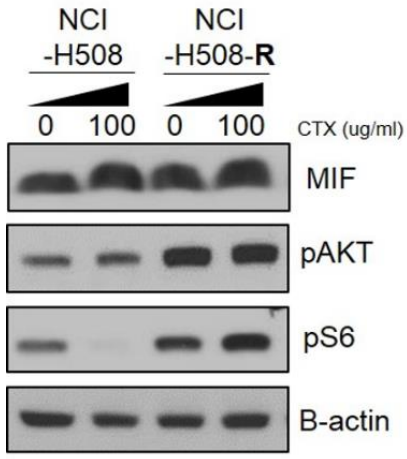

Figure 8. (D) Secreted MIF levels were measured in NCI-H508^{WT} and NCI-H508_CR^{Q61L} cells ELISA. **(E)** Western blot analysis of the AKT signaling pathway was observed in parental and NCI-H508_CR^{Q61L} cells after cetuximab treatments.

F

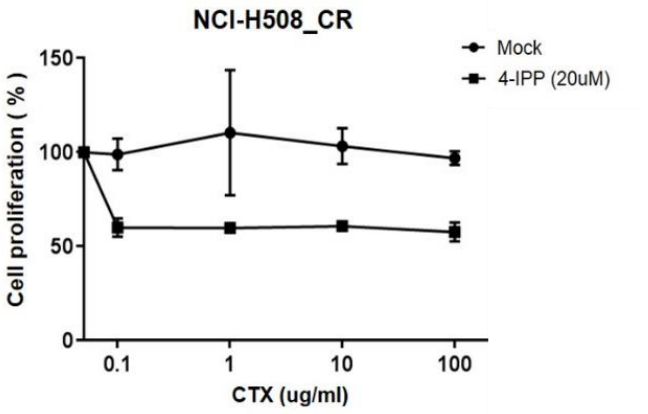

G

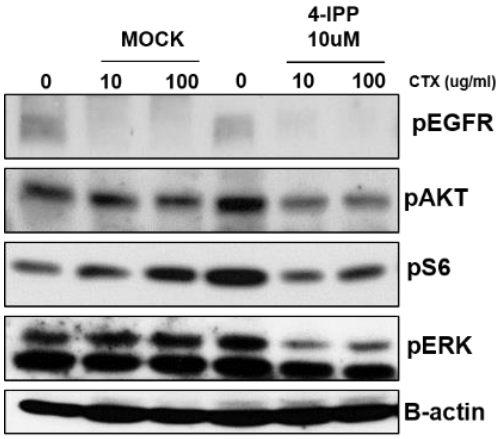

Figure 8. (F) 20uM 4-IPP was treated for 72hrs with increasing doses of cetuximab (0.1, 1, 10, and 100 μg/mL) to NCI-H508_CR^{Q61L} cells. Cell viability was assayed by the MTT assay. Data points represent means ± SD of three independent experiments. **(G)** Cetuximab (10 and 100 μg/mL) and 4-IPP 10uM treated to NCI-H508_CR^{Q61L} cells and signaling was observed by western-blotting.

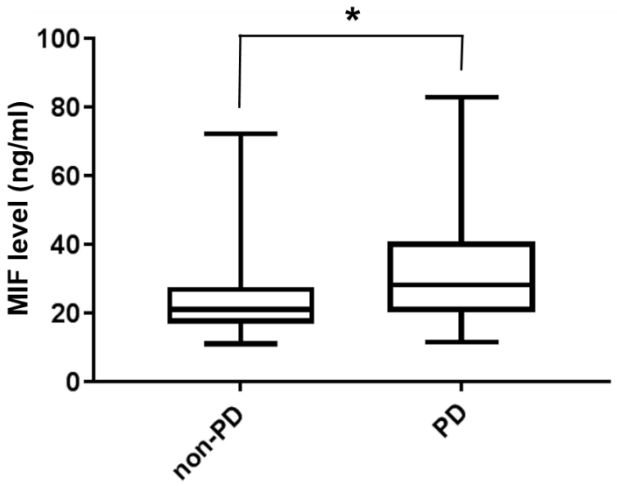

Figure 9. MIF secreted levels of base line serum in KRAS^{WT} patient groups.

The level of MIF is elevated in PD patient samples MIF levels in serum of 19 KRAS^{WT} and 20 KRAS^{MT} patients were measured by human MIF ELISA. Data represent means ± SD of two independent experiments, P=0.12.

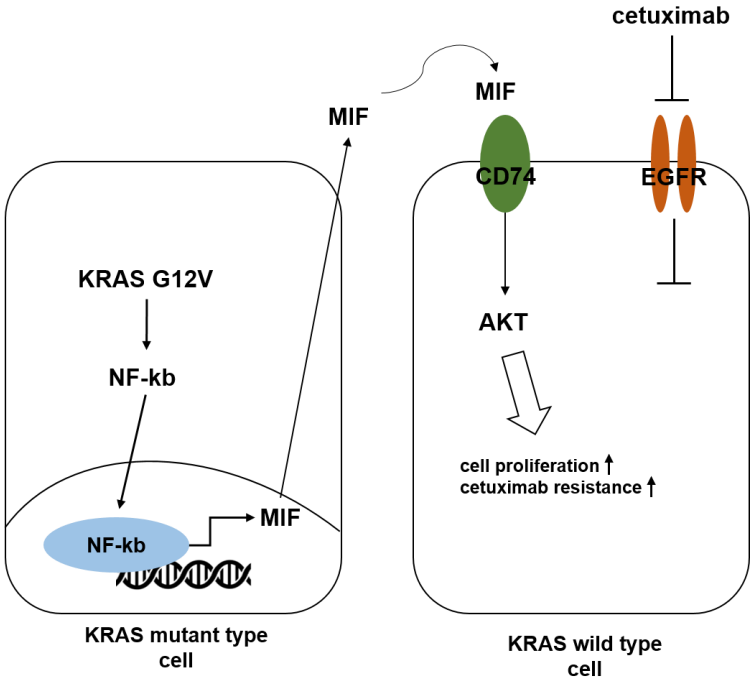

Figure 10. In KRAS mutant-type cells, oncogenic KRAS activates NF-kB transcription factor and it was translocated from cytosol to nucleus. Activated NF-kB increases MIF transcription level in the nucleus and regulated MIF is secreted out of the cells. Secreted MIF acts as ligand for CD74 receptor and activates AKT signaling pathway in KRAS wild-type cells, consequently, cetuximab block the EGFR signaling but cetuximab resistance occurs by activated AKT signaling. It shows direct evidence that paracrine-MIF leads to cetuximab resistance through AKT signaling activation bypass from EGFR signaling.

DISCUSSION

This study provides evidence that colorectal cancer cells carrying KRAS mutation affect to the surrounding cells including $KRAS^{WT}$ cells promoting tumor progression and cetuximab resistance. My finding was that oncogenic-KRAS mediates cell to cell interactions that are crucial to the promotion of tumor growth, proliferation, invasion ability, and cetuximab resistance in surrounding $KRAS^{WT}$ cells through paracrine-signal by secreted MIF (Figure 10). Overall, my results support the possibility of paracrine in protection of $KRAS^{WT}$ cells from cetuximab through activated AKT signaling by secreted MIF from $KRAS^{MT}$ cells. Intra-tumoral heterogeneity of malignant tumor cells of human colorectal cancer has been well reported [26]. Most cancers initially respond to drug treatment, however, they often relapse with the outgrowth of cancer cells that are no longer sensitive to the therapy because of the heterogeneity [27, 28]. The role of tumor microenvironment during initiation and progress of carcinogenesis is realized as critical importance. Tumor microenvironment includes stromal fibroblasts, infiltrating immune cells, the blood and lymphatic vascular networks, and the extracellular matrix [29]. Tumor cells produce a variety of growth factors, and chemokines that enhance the proliferation and invasion of the tumor. Furthermore, reported data showed that conditioned medium from stromal cells provided

protection only if it was collected from cells grown in co-culture with myeloma cells [30]. This indicates that a dynamic interaction between tumor cells and their stroma is required to produce the soluble factors that mediate drug resistance. Therefore, I investigated whether secreted cytokine from $KRAS^{MT}$ cells affects on the surrounding cells including $KRAS^{WT}$ cells in tumor microenvironments. Furthermore, I have hypothesized that if there are existence of an only few $KRAS^{MT}$ cell populations although KRAS mutation is not detected in colorectal tumor burden due to showing tumor heterogeneity, the arounding $KRAS^{WT}$ cells may be affected by $KRAS^{MT}$ cells. Above all, I observed that tumor cell proliferation, growth, wound healing ability, and invasion ability were promoted when I treated CM to $KRAS^{WT}$ cells (Figure 2). In addition, cetuximab targeting EFGR resistance were appeared after cetuximab treatment with CM in $KRAS^{WT}$ cells (Figure 3). I suggested that these results showed cytokine-dependent in the CM. Previous reports discovered that acquired cetuximab resistant colorectal cancer cells secreted TGF alpha and amphiregulin, which protect the surrounding cells from cetuxiamb [31]. However, original tumor heterogeneity was not reflected in this study. Macrophage migration inhibitory factor (MIF) which target gene that I discovered by proteomic analysis is one of the first cytokine to be discovered. MIF is relatively small size (12.5kDa) lacking conventional N-terminal leader sequence and is therefore released from the cell by leaderless secretion pathway

[32]. MIF is capable of promoting pro-tumorigenic activity in tumor stromal cells including the endothelia and tumor-associated immune cells within tumor microenvironment. Yet, the mechanism by which transcription factor regulated MIF by KRAS mutation remains incompletely characterized. In this study, I observed that the expression of MIF was regulated by NF-kB transcription factor following KRAS mutation status (Figure 7). Elevated expression of MIF may play an important role in tumor growth and survival by stimulating a paracrine-signaling. This may characterize a tumor that is KRAS mutation-induced MIF dependent and, therefore, particularly sensitive to the ability of cetuximab to block AKT signaling. Cetuximab treatments can block the EGFR signaling (RAF-MEK-ERK signals) thereby cell proliferation is inhibited in $KRAS^{WT}$ cells. My results showed that EGF receptor could be blocked by cetuximab, however, PI3K/AKT signaling is activated by MIF therefore the cell proliferation could not be protected from cetuximab treatments under $KRAS^{WT}$ cells surrounded by $KRAS^{MT}$ cells. However, it was restored by MIF inhibitor 4-IPP co-treated with cetuxiamb (Figure 5). There are non-responder groups to cetuximab with no detected KRAS mutations [33]. Thus, MIF expression contributes to tumorigenesis in $KRAS^{WT}$ cells located around $KRAS^{MT}$ cells and increases in resistance to cetuximab treatment, raising the possibility that treatment of KRAS wild-type tumors with targeting MIF may be more effective than cetuximab treatment alone. These data have provided a

foundation for a rational approach to the targeted therapy of cetuximab in patients with tumors that had KRAS wild-type. KRAS wild-type colorectal tumors are often sensitive to EGFR blockade cetuximab, but almost always develop resistance within several months of initiating therapy [34]. Acquired resistance develops over time as a result of sequential genetic changes that ultimately culminate in complex therapy-resistant phenotypes. Development of resistance to cetuximab is due to rare cells with KRAS mutations pre-exist at low populations in tumors, which are detected as KRAS wild-type [35]. Eventually, cetuximab acquired resistance occurs in remaining population of the tumor cells harboring KRAS mutation after elimination of KRAS wild-type cells by cetuximab. I developed cetuximab acquired resistant cells with NCI-H508^{WT} cells and investigated cetuximab resistance mechanism related with MIF expression. Cetuximab-resistant NCI-H508_CR^{Q61L} cells acquired KRAS Q61L mutation and I found that acquired cetuximab resistance was associated with enhanced MIF gene expression in NCI-H508-CR^{Q61L} cells increasing AKT signaling. Therefore, these findings suggest that attractive characteristics of MIF monitoring in the circulation is expected not only the aspect of cetuximab resistant predictive biomarker including the ease of application of ELISA and the noninvasive nature of repeated sample acquisition but also as the therapeutic target who appears secondary mutation following cetuximab treatment in KRAS wild-type patients. Monitoring of MIF may be a

possible potential marker to use of cetuximab in patients who are carrying wild-type KRAS in certuximab non-response group.

In summary, my results provide insights into the relationship between oncogenic KRAS-derived MIF and cetuximab resistance in tumor microenvironments. In addition, the level of plasma MIF has the potential to serve as a non-invasive serum biomarker to predict response to treatment of EGFR inhibitor, particularly those with wild-type KRAS and highly secreted MIF in cetuximab non-response group

REFERENCE

1. Siegel, R.L., et al., *Colorectal cancer statistics, 2017.* CA Cancer J Clin, 2017. **67**(3): p. 177-193.
2. Fearon, E.R., *Molecular genetics of colorectal cancer.* Annu Rev Pathol, 2011. **6**: p. 479-507.
3. Prenen, H., L. Vecchione, and E. Van Cutsem, *Role of targeted agents in metastatic colorectal cancer.* Target Oncol, 2013. **8**(2): p. 83-96.
4. Cancer Genome Atlas, N., *Comprehensive molecular characterization of human colon and rectal cancer.* Nature, 2012. **487**(7407): p. 330-7.
5. Bos, J.L., *ras oncogenes in human cancer: a review.* Cancer Res, 1989. **49**(17): p. 4682-9.
6. Bos, J.L., et al., *Prevalence of ras gene mutations in human colorectal cancers.* Nature, 1987. **327**(6120): p. 293-7.
7. Downward, J., *Targeting RAS signalling pathways in cancer therapy.* Nat Rev Cancer, 2003. **3**(1): p. 11-22.
8. Artale, S., et al., *Mutations of KRAS and BRAF in primary and matched metastatic sites of colorectal cancer.* J Clin Oncol, 2008. **26**(25): p. 4217-9.
9. Wood, L.D., et al., *The genomic landscapes of human breast and colorectal cancers.* Science, 2007. **318**(5853): p. 1108-13.
10. Goldie, J.H. and A.J. Coldman, *A mathematic model for relating the drug*

sensitivity of tumors to their spontaneous mutation rate. Cancer Treat Rep, 1979. **63**(11-12): p. 1727-33.

11. Goldie, J.H. and A.J. Coldman, *Quantitative model for multiple levels of drug resistance in clinical tumors.* Cancer Treat Rep, 1983. **67**(10): p. 923-31.
12. Ciardiello, F. and G. Tortora, *EGFR antagonists in cancer treatment.* N Engl J Med, 2008. **358**(11): p. 1160-74.
13. Misale, S., et al., *Emergence of KRAS mutations and acquired resistance to anti-EGFR therapy in colorectal cancer.* Nature, 2012. **486**(7404): p. 532-6.
14. Bedard, P.L., et al., *Tumour heterogeneity in the clinic.* Nature, 2013. **501**(7467): p. 355-64.
15. Junttila, M.R. and F.J. de Sauvage, *Influence of tumour micro-environment heterogeneity on therapeutic response.* Nature, 2013. **501**(7467): p. 346-54.
16. Tredan, O., et al., *Drug resistance and the solid tumor microenvironment.* J Natl Cancer Inst, 2007. **99**(19): p. 1441-54.
17. Meads, M.B., R.A. Gatenby, and W.S. Dalton, *Environment-mediated drug resistance: a major contributor to minimal residual disease.* Nat Rev Cancer, 2009. **9**(9): p. 665-74.
18. Balkwill, F., *Cancer and the chemokine network.* Nat Rev Cancer, 2004. **4**(7): p. 540-50.

19. Gregory, J.L., et al., *Macrophage migration inhibitory factor induces macrophage recruitment via CC chemokine ligand 2.* J Immunol, 2006. **177**(11): p. 8072-9.

20. Bucala, R. and S.C. Donnelly, *Macrophage migration inhibitory factor: a probable link between inflammation and cancer.* Immunity, 2007. **26**(3): p. 281-5.

21. He, X.X., et al., *Macrophage migration inhibitory factor promotes colorectal cancer.* Mol Med, 2009. **15**(1-2): p. 1-10.

22. Chen, W.T., et al., *Identification of biomarkers to improve diagnostic sensitivity of sporadic colorectal cancer in patients with low preoperative serum carcinoembryonic antigen by clinical proteomic analysis.* Clin Chim Acta, 2011. **412**(7-8): p. 636-41.

23. Ku, J.L. and J.G. Park, *Biology of SNU cell lines.* Cancer Res Treat, 2005. **37**(1): p. 1-19.

24. Dessein, A.F., et al., *Autocrine induction of invasive and metastatic phenotypes by the MIF-CXCR4 axis in drug-resistant human colon cancer cells.* Cancer Res, 2010. **70**(11): p. 4644-54.

25. Li, G.Q., et al., *Macrophage migration inhibitory factor regulates proliferation of gastric cancer cells via the PI3K/Akt pathway.* World J Gastroenterol, 2009. **15**(44): p. 5541-8.

26. Brattain, M.G., et al., *Heterogeneity of human colon carcinoma.* Cancer Metastasis Rev, 1984. **3**(3): p. 177-91.

27. Marusyk, A., V. Almendro, and K. Polyak, *Intra-tumour heterogeneity: a looking glass for cancer?* Nat Rev Cancer, 2012. **12**(5): p. 323-34.

28. McGranahan, N. and C. Swanton, *Biological and therapeutic impact of intratumor heterogeneity in cancer evolution.* Cancer Cell, 2015. **27**(1): p. 15-26.

29. Allinen, M., et al., *Molecular characterization of the tumor microenvironment in breast cancer.* Cancer Cell, 2004. **6**(1): p. 17-32.

30. Nefedova, Y., T.H. Landowski, and W.S. Dalton, *Bone marrow stromal-derived soluble factors and direct cell contact contribute to de novo drug resistance of myeloma cells by distinct mechanisms.* Leukemia, 2003. **17**(6): p. 1175-82.

31. Hobor, S., et al., *TGFalpha and amphiregulin paracrine network promotes resistance to EGFR blockade in colorectal cancer cells.* Clin Cancer Res, 2014. **20**(24): p. 6429-38.

32. Bernhagen, J., et al., *Purification, bioactivity, and secondary structure analysis of mouse and human macrophage migration inhibitory factor (MIF).* Biochemistry, 1994. **33**(47): p. 14144-55.

33. Khambata-Ford, S., et al., *Expression of epiregulin and amphiregulin and*

K-ras mutation status predict disease control in metastatic colorectal cancer patients treated with cetuximab. J Clin Oncol, 2007. **25**(22): p. 3230-7.

34. Karapetis, C.S., et al., *K-ras mutations and benefit from cetuximab in advanced colorectal cancer.* N Engl J Med, 2008. **359**(17): p. 1757-65.

35. Diaz, L.A., Jr., et al., *The molecular evolution of acquired resistance to targeted EGFR blockade in colorectal cancers.* Nature, 2012. **486**(7404): p. 537-40.

국문 초록

암은 intra-heterogeneity의 특성을 보이며, 다양한 돌연변이를 보이는 세포들로 구성되어 있다. 이는 표적치료를 하는데 있어 어려운 요인 중에 하나로, 암 미세 환경을 통해 세포에서 분비되는 사이토카인에 의한 상호작용을 통해 야기된다고 알려져 있다. 따라서 본 연구에서는 암 내에서, KRAS 돌연변이 세포가 분비한 사이토카인이 암 미세환경을 통해 KRAS 정상세포에 미치는 영향을 보고자 하였다. KRAS 돌연변이 세포주를 배양한 conditioned media (CM)를 KRAS 정상 세포주에 처리 하였을 때, 종양 진행에 관련된 특성들 (세포 성장, 콜로니 형성 능력, 상처 치유 능력, 그리고 침습 능력)이 증진됨을 확인 하였다. 또한 세툭시맙에 민감도를 보이는 KRAS 정상 세포주에서 CM의 처리에 따라 세툭시맙에 대한 내성이 야기됨을 확인 하였다. 이는 단백질 분석기법을 통해 CM내의 MIF 유전자가 KRAS 돌연변이 세포주에서 높게 발현하고 있음을 발견하였고, 더 나아가 KRAS 정상 세포주에 비해 KRAS 돌연변이 세포주에서 상대적으로 많이 분비되는 것을 관찰할 수 있었다. 이에 대한 메카니즘을 분석한 결과 KRAS 돌연변이 세포주내에서 KRAS 돌연변이에 의해 활성화된 NF-kB 전사 인자가, 핵내의 MIF의 전사를 조절하여 분비 시킴을 밝혀내었다. 또한 분비된 MIF는 paracrine-signaling을 통하여 KRAS 정상 세포주의 CD74 수용체

를 통해 AKT signaling을 활성화시켜, 세툭시맙에 대한 내성을 야기함을 밝혀내었다. 마지막으로 KRAS 정상세포주를 이용하여 세툭시맙 획득 내성 세포주를 구축하였을 때 KRAS Q61L 돌연변이가 발생된 것을 확인 하였고, MIF 유전자의 발현과 분비가 증가 하였음을 관찰하였다. 이를 토대로 MIF가 세툭시맙 내성 예측 마커로서의 가능성을 확인하기 위하여, 세툭시맙을 투여 받는 KRAS 정상 환자군의 혈액 샘플에서 MIF의 분비량을 측정해 보았다. 세툭시맙 투여 후 진행병변 (PD)이 발생한 환자군의 base line 샘플에서 대조군에 비해 MIF의 분비가 증가되어 있음을 ELISA를 통하여 관찰하였다.

결론적으로 본 논문에서는 KRAS 돌연변이 세포주에서 분비된 MIF가, KRAS 정상 대장암 세포주에 세툭시맙에 대한 내성을 야기함을 관찰 하였고, 이에 대한 메카니즘을 처음으로 규명 하였다. 또한 더 나아가 MIF는 비침습적인 방법을 통해 KRAS 정상 대장암 환자에서 세툭시맙 내성 예측 바이오 마커로서의 사용 가능성을 시사하고 있다.

주요어 : 대장암, KRAS 돌연변이, 암 미세환경, MIF, 세툭시맙

학번 : 2014-31287